AD658721

NRL Report 6564

Stress-Corrosion Cracking Characteristics of Alloys of Titanium in Salt Water

July 21, 1967

NAVAL RESEARCH LABORATORY
Washington, D.C.

53

NRL Report 6564

Stress-Corrosion Cracking Characteristics of Alloys of Titanium in Salt Water

R. W. Judy, Jr. and R. J. Goode

Strength of Metals Branch
Metallurgy Division

July 21, 1967

NAVAL RESEARCH LABORATORY
Washington, D.C.

CONTENTS

ABSTRACT

The salt water stress-corrosion cracking (SCC) characteristics have been determined for a large number of titanium alloys representatives of commercial production. These data were compiled as part of an NRL program directed to determining the underlying principles of SCC in metals and to establishing procedures for improving the SCC resistance of these metals as well as learning to tolerate the problem where it exists.

The SCC resistance was determined using a precracked cantilever bend specimen with analysis by fracture mechanics techniques. The test results for the spectrum of alloys and weldments studied indicate that no correlation with mechanical properties exists, which makes precise prediction of SCC properties of particular alloys difficult, if not impossible.

The data obtained provide guideline information for programs similar in nature to the NRL program as well as for alloy development, design and materials selection, and specifications and quality control.

PROBLEM STATUS

This is an interim report; work is continuing.

AUTHORIZATION

This research was supported by the Advanced Research Projects Agency of the Department of Defense under ARPA Order No. 878, NRL Problem No. M04-08B, and was monitored by the Naval Research Laboratory under Contract Nos. Nonr-610(09), Nonr-760(31), and NOOO14-66-CO365.

The research was also supported by the Deep Submergence Systems Project of the Department of Defense SP-01426, NRL Problem No. F01-17, PO 7-0001 TASK 11894.

Manuscript submitted March 7, 1967.

STRESS-CORROSION CRACKING CHARACTERISTICS OF ALLOYS OF TITANIUM IN SALT WATER

INTRODUCTION

Titanium alloys, as a group, have several properties which make them desirable for use in naval applications, primarily as structural materials for pressure vessels and hull material for research type submersibles. High strength-to-density ratio, good fracture-toughness characteristics, good weldability, nonmagnetic characteristics, and good general corrosion and erosion characteristics are the principle features of many of the alloys. However, a number of the titanium alloys are sensitive to stress-corrosion cracking (SCC) in salt water if the proper set of conditions exists.

Three separate and distinct phases of failure by stress-corrosion cracking exist for other materials such as steels and aluminum alloys: (a) the formation of small pits by erosion or corrosion attack, (b) the formation and propagation of a sharp crack at the bottom of the pits (SCC), and (c) rapid unstable crack propagation when the crack has grown to sufficient size. Since smooth specimens of titanium alloys are not affected by exposure to aqueous environments, their sensitivity to stress-corrosion cracking in salt water was not discovered until a test specimen which included a sharp flaw was designed.

For stress-corrosion cracking to occur in titanium alloys, it has been shown (1) that three conditions must exist simultaneously: a stress of sufficient magnitude, a flaw of sufficient size and acuity, and an aggressive environment. Stress level and flaw size can be combined and expressed in terms of the fracture mechanics stress intensity factor K_I, and expressing SCC resistance in terms of K provides some degree of translation to expected structural performance. Studies based on the fracture mechanics approach have been conducted at the Naval Research Laboratory on a large number of commercially produced titanium alloys as part of a program directed to determining the underlying principles related to SCC sensitivity in metals and to establishing procedures for improving their SCC resistance as well as learning how to tolerate the problem where it exists.

The results are presented for the whole spectrum of titanium alloy materials studied, to insure that maximum benefits are derived not only by those concerned with similar programs but also by those concerned with developing alloys with high SCC resistance, specifying current production alloys for use in structures, and providing information which can be utilized in design. It must be emphasized that the SCC studies are continuing and that this report is considered the first edition of a catalog directed to providing the widest compendium of SCC information on advanced high and ultrahigh strength structural metals.

EXPERIMENTAL PROCEDURE

The test method used in this study was the precracked-cantilever-beam test introduced by B. F. Brown (2). In this test a bar, of square or rectangular cross section, containing a fatigue-crack flaw is loaded in bending in the presence of a 3-1/2-wt-% NaCl solution. The lowest stress intensity level, denoted K_{Iscc}, at which SCC can definitely be shown to occur is found by bracketing techniques. To accomplish this a specimen is loaded to a known K_I level after the salt water solution is applied. Loading rates are

quite rapid, usually being less than 5 seconds until the full load is applied. If the specimen does not break in 1 hour, the load is increased by steps at regular intervals until fracture occurs, the time to fracture being recorded. The initial K_I level is denoted as "No Break" and is used to bracket K_{Iscc}.

The data is displayed on a plot of K_I versus time to fracture, K_{Iscc} being indicated as the lowest K_I line above which SCC has been shown to occur. Brackets or limit values on data points are used to indicate that the fatigue crack was irregular. The limits are the maximum and minimum K_I values which can be calculated from the irregular fatigue crack; the center data point is the numerical average of these limits.

Comparison of K_{Iscc} with K_{Ix}, the stress intensity required for fracture in air (designated "Dry"), gives an indication of the relative resistance of an alloy to SCC for the specimen geometry used. The test specimen, along with the equation used to calculate K_I values (3), is shown schematically in Fig. 1. A typical fractured specimen of an alloy quite sensitive to SCC is shown in Fig. 2, with the fatigue, SCC, and fast fracture zones illustrated. A typical SCC test machine is shown in Fig. 3.

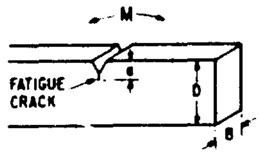

$$K_I = \frac{4.12\, M \sqrt{\frac{1}{\alpha^3} - \alpha^3}}{BD^{3/2}}$$

$$\alpha = 1 - \frac{a}{D}$$

Fig. 1 - Schematic of SCC specimen and equation for calculating the stress intensity factor K_I

Fig. 2 - A typical fractured SCC specimen of a titanium alloy

The specimens tested varied in cross-sectional dimensions; the dimensions of the specimens for each particular alloy are given in the tables contained in this report. In some cases shallow side grooves were employed to suppress shear lip formation; the side groove depths are also given in the tables.

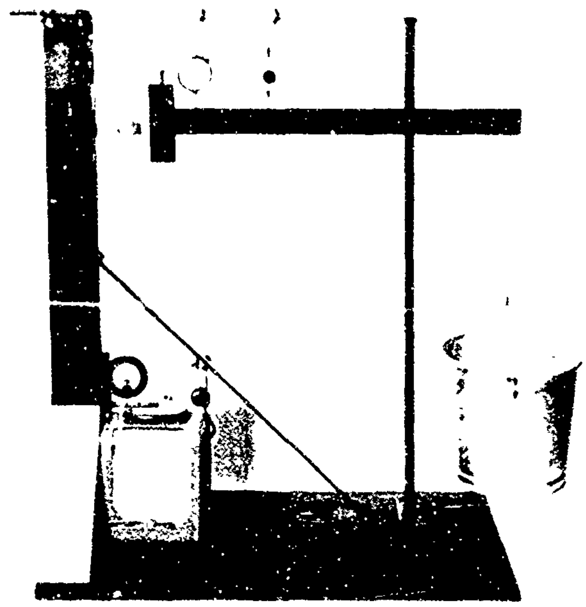

Figure 5 - Apparatus used for SCC tests

In testing weldments of titanium alloy plate, it was desirable to obtain SCC information at several points in the weldment. For this reason, tests were conducted on specimens that have the notched test section located at the weld centerline at the fusion line, and at various points in the heat-affected-zone (HAZ). Since welded plate is difficult and expensive to fabricate, the dry value K_{Ix} was not determined in all cases.

RESULTS

Environmental cracking data for some titanium alloy base plates along with some mechanical properties of the alloys tested are shown in Table 1. Figures 6 through 76 show the characterization curves for the same alloys. Except as noted all specimens were taken from 1-inch plate in the as-received (mill-annealed) condition and had low interstitial contents (below 0.08% O_2). Table 2 and Figs 77 through 90 illustrate SCC characterization data for weldments of some of the base plate material. Particular information concerning types of weldments and notch locations are also given

A summary chart showing the relative sensitivities of titanium alloys in several plate-thicknesses and as-received and heat-treated conditions is shown in Fig. 4. This chart is a plot of yield strength (YS) versus K_{Iscc} and is referenced by lines of constant critical flaw depths. These reference lines represent the flaw depth necessary to cause crack extension due to SCC at yield strength loading for the case of the 10:1 flaw (width of flaw = 10 times flaw depth) — presumably the worst possible case (4). The critical flaw depth (a) is calculated by the formula $a = 0.2(K_{Iscc}/YS)^2$.

At the beginning of the SCC studies on titanium alloys, it was assumed that laboratory test results with a 3-1/2-wt-% salt water environment would not significantly differ from results obtained with a fresh sea water environment. This assumption was based

Table 1
Stress Corrosion Cracking Characteristics of Some Titanium Alloys

Titanium Alloys	Code	YS (ksi)	DWTT (ft-lbs)	K_{Ic} (ksi √in)	K_{Iscc} (ksi √in)	Specimen Dimensions Depth (in)	Width (in)	Side Groove Depth (in)	Remarks
5Al-2 5Sn	3	112	2750	130	50	1	3 4	1 10	
5Al-2 5Sn	7	125 5	2000	119	50	1	3 4	1 8	
13V-11Cr-3Al	9	128 5	1000	88	28	1	3 4	1 8	
Unalloyed	17	3	500	69	40	1	3 4	1 32	High interstitial
5Al-2 5Sn	18	--	1750	112	50	1	3 4	1 10	
5Al-2 5Sn	18	114 7	1750	128	72	1	11 16	1 8	
8Al 1Mo-1V	19	120 4	--	88	23	1	1 2	-	1700 F 1 hr AC 1200 F 2 hr WQ
8Al-1Mo-1V	19	107 9	--	112	28	1	1 2	--	1825 F 1 hr AC
6Al-4Sn-1V	20	131 4	2250	114	42	1	11 16	1 32	1825 F 1 hr WQ
6Al-6V-2 5Sn	21	179 6	--	55	21	1	3 4		1100 F 2 hr AC 1550 F 1 hr WQ- 900 F 4 hr AC
6Al-2Mo	22	124 4	3333	122	102	1	11 16	1 32	1750 F 1 hr AC 1100 F 4 hr WQ
8Al-2Cb-1Ta	23	113	1750	102	31	1	3 4	1 32	
6Al-2Sn-1Mo-1V	25	100	2250	109	70	1	3 4	1 10	
6Al-4V	27	120	931	88	67	1	11 16	1 32	
6Al-4V	32	121	660	101	80	1	3 4	1 10	High interstitial
6 5Al-5Zr-1V	36	127	1480	99	49	1	3 4	1 16	
6Al-2Sn-1Mo-1V	37	121 5	1660	112	96	1	3 4	--	
7Al-2Cb-1Ta	39	106	2086	105	43	1	11 16	--	
6Al-6Zr-1Mo	41	102	2646	106	102	1	1 2	1 16	
7Al-3Mo	46	103 9	2808	128	45	1	-	-	
3Al	52	71 3	5000	81	64	1	1 2	1 16	
6Al-4Zr 2Mo	55	121 4	1478	117	46	1	3 4	1 32	
6Al-4V	56	123 7	--	116	95	1 2	1 2	-	
5Al-2 5Sn	57	113 6	--	112	39	1 2	1 2	-	
7Al-2Cb-1Ta	58	113 0	--	42	40	1 2	1 2	-	
6Al-2Mo	59	123 0	--	116	76	1 2	1 2	--	
7Al-12Zr	62	110 5	870	108	42	1	3 4	1 8	Laminate structure
6Al-4V-2Sn	67	115 8	1173	97	88	1	3 4	1 8	
6Al-4Zr-2Sn-0 5Mo-0 5V	68	113 5	1784	124	40	1	3 4	1 8	
10Mo-5 4Sn	69	115	1905	129	128	1	1 2	1 16	1200 F 48 hr WQ
7Al-2Cb-1Ta	70	102 4	2114	110	63	1	1 2	--	Distilled water
7Al-2Cb-1Ta	70	100 8	2294	118	40	1	11 16	--	Sea water
7Al 2 5Mo	71	113 5	1751	112	88	1	3 4	1 32	
7Al-2Cb-1Ta	72	102 8	2174	134	45	1	5 8	1 10	2200 F lge reduction AC
7Al-2Cb-1Ta	73	103	2206	130	56	1	5 8	1 10	
7Al-2Cb-1Ta	74	-	2206	122	50	1	5 8	1 10	Planetary rolled
7Al-2Cb-1Ta	75	--	2902	118	43	1	5 8	1 10	
7Al-3Cb-2Sn	76	108 5	2026	146	75	1	5 8	1 10	
7Al-2Cb-1Ta	78	--	1281	129	88	1	1 2	1 16	
6Al-2Mo-2V-2Sn	80	120	1540	99	96	1	3 4	1 10	
7Al-1Mo-1V	88A	--	--	94	90	1 2	1 2	1 16	1750 F 1 hr vac FC
7Al-1Mo-1V	88B	--	--	90	78	1 2	1 2	1 16	
7Al-1Mo-1V	88C	105 6	2443	111	80	1	1 2	1 32	
7Al-1Mo-1V	88D	106 4	2026	122	92	1	1 2	1 32	1850 F 1 hr He cool
7Al-1Mo-1V	88E	119 8	1228	117	90	1	1 2	1 32	1 [illegible]0 F 1 hr He cool
7Al-1Mo-1V	88	113 7	--	118	42	1	3 4	1 32	1800 F 1 hr He cool
7Al-2Cb-1Ta	89	110 6	2146	119	45	1	5 8	1 8	
5Al-2V-2Mo-2Sn	90	112 7	1723	108	100	1	3 4	1 10	
6Al-4V	91	104 9	1228	118	90	1	3 4	1 10	
6Al-6V-2Sn-1Cu-0 5Fe	92	122 1	681	111	96	1	3 4	1 10	
6Al-6V-2Sn-1Cu-0 5Fe	92	120 1	--	102	78	1	3 4	1 32	1660 F 1 hr He cool
6Al-3V-1Mo	93	116 5	1173	116	110	1	3 4	1 10	
6Al-3V-1Mo	93	--	--	112	98	1	3 4	1 32	1850 F 1 hr He cool
7Al-2 5Mo	94	119 2	1540	101	80	1	1 2	1 32	
7Al-2 5Mo	94B	99 0	2086	118	93	1	1 2	1 32	1800 F 1 hr He cool
7Al-2 5Mo	94	108	--	123	92	1	3 4	1 32	1800 F 1 hr He cool
6Al-4V	95	-	811	94	68	1	1 2	1 32	ELI Grade (0 12% O_2)
6Al-4V (ELI)	95	--	--	112	84	1	3 4	1 32	1850 F 1 hr He cool
6Al-2Cb-1Ta-0 8Mo	96	--	2384	117	98	1	1 2	1 32	
11Mo-5Sn-5Zr	97	100 5	1021	117	94	1	1 2	1 32	
3 5Al	98	74 0	397	90	80	1	1 2	1 32	
3 5Al	98	70 9	4724	101	80	1	1 2	1 32	1660 F 1 hr He cool
6Al-4V	100E	--	1052	107	100	1	1 2	1 32	
6Al-2Mo	R1	117 6	1601	107	94	1	3 4	1 32	
6Al-4V-2Mo	R2	126 0	1052	96	82	1	3 4	1 32	
6Al-6V-2Sn-2Mo	R4	138 2	514	71	65	1	3 4	1 32	
6Al-6V-2Sn-2Mo	R4	126 8	681	91	82	1	3 4	1 32	1660 F 2 hr He cool
Unalloyed - A-70	--	78-84	--	65	44	1 2	1 4	--	High interstitial
7Al-2Cb-1Ta	--	105-110	--	100	35	7 8	1 2	--	Mat'l from DTMB NSRDC
8Al-1Mo-1V	--	130	--	54	19	1 8	--	--	
6Al-4V	--	165	--	64	55	3 4	1 10	--	Minuteman Casing Mat l

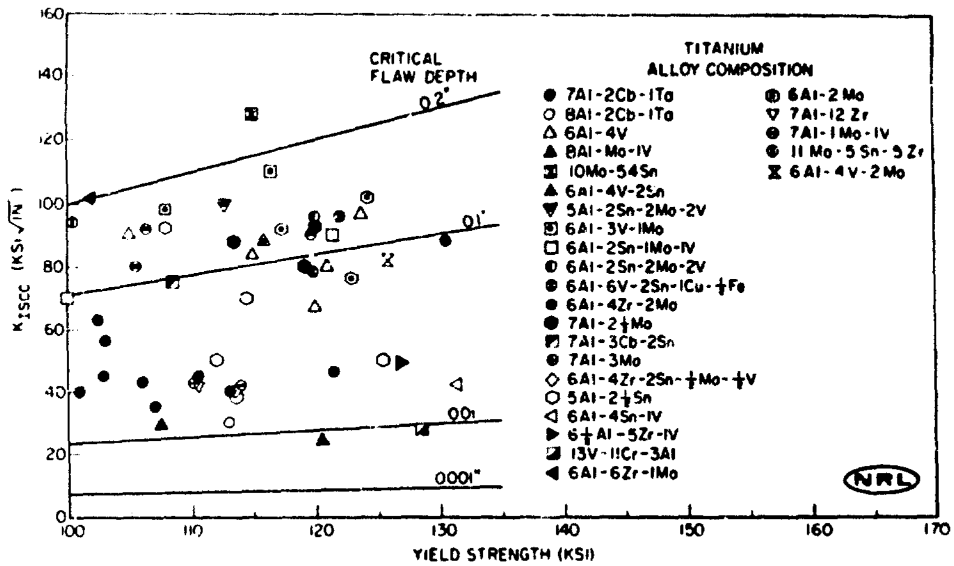

Fig. 4 - Stress corrosion cracking resistance index for titanium alloys in 3.5% salt water

on the observed rapid crack propagation rate and consequent short time required for complete fracture of the titanium alloy specimen at K_I levels very near K_{Iscc}. To test this assumption several specimens of a Ti-7Al-2Cb-1Ta alloy (coded T89) (an alloy very sensitive to SCC) were tested at NRL's Key West, Florida, facility using fresh flowing sea water as the environment. The same testing equipment and procedures were used in each case, the only difference being that specimens having 1/8-in.-deep side grooves were tested in the laboratory solution, whereas the specimens tested in sea water were not side-grooved. Previous tests indicated that similar results could be expected in the laboratory for both specimen types for titanium alloys having low resistance to SCC.

Figure 5 shows the results of both tests, which were essentially the same. Both the K_{Iscc} values and the subcritical crack growth portion of the curves (time to fracture) agreed very closely, which indicates that the original assumption of similarity of SCC results in both environments seems to be valid. For further confirmation other studies of alloys which are not extremely sensitive to SCC will be made.

Some investigators (5) have reported that the presence of molybdenum as an alloying addition generally improves the SCC resistance of titanium alloys. This is borne out in tests of the Ti-6Al-2Cb-1Ta-0.8Mo alloy (T96), which is similar to the highly SCC sensitive Ti-7Al-2Cb-1Ta alloy. The substitution of 0.8% Mo for 1.0% Al resulted in a K_{Iscc} level of 98 ksi $\sqrt{\text{in.}}$ for the T96 alloy, which is considerably higher than the highest K_{Iscc} level of any Ti-7Al-2Cb-1Ta alloy tested. However, other molybdenum containing alloys such as 7Al-1Mo-1V (T88) and 8Al-1Mo-1V (T19) were shown to be quite SCC sensitive.

SCC tests of various types of weldments indicate that these alloys can be welded without a severe reduction in SCC resistance. A study of eight different MIG weldments (Table 2) showed that values of K_{Iscc} generally decreased for welded material compared to base plate and that solution heat-treatment in the alpha and beta range improved the characteristics of the welded plate.

Table 2
Stress Corrosion Characteristics of Titanium Alloy Weldments

Titanium Alloy	Code	YS (ksi)	DWTT (ft-lb)	K_{Ic} (ksi $\sqrt{in}$)	K_{Iscc} (ksi $\sqrt{in}$)	Type Weldment*	Notch Location: Dist from Fusion Line (in)	Specimen Dimensions: Depth (in)	Specimen Dimensions: Width (in)	Specimen Dimensions: Side Groove Depth (in)	Remarks
6Al 2Mo	T-22	--	--	--	82	EB	0 30	1	3 4	1 8	
		--	--	--	87	EB	0 90				
		--	--	--	88	EB	1 20				
		-	--	--	89	EB	1 50				
6Al-2Mo	T-22	--	--	--	70	MIG	0 063	1	3 4	1 8	
		--	--	--	74	MIG	0 125				
		--	--	--	83	MIG	0 188				
		--	--	--	79	MIG	0 200				
		--	--	--	84	MIG	0 250				
6Al-4V	T-27	--	--	--	81	EB	0 60	1	3 4	1 8	
		--	--	--	94	EB	0 90				
		--	--	--	85	EB	1 20				
		--	--	--	100	EB	1 50				
6Al-4V	T-27	--	--	--	100	MIG	℄ Weld	1	3 4	1 8	
		--	--	--	101	MIG	0				
		--	--	--	91	MIG	0 063				
		--	--	--	102	MIG	0 196				
7Al-2Cb-1Ta	T-78	-	-	-	65	EB	0	1	5 8	--	
		--	--	--	59	EB	0 10				
		--	--	--	61	EB	0 30				
		--	--	--	5[illegible]	EB	0 40				
		--	--	--	64	EB	0 50				
		--	--	--	55	EB	0 60				
		--	--	--	50	EB	0 70				
7Al-2Cb 1Ta	T-78	--	--	--	47	MIG	℄	1	3 4	-	
		--	--	--	45	MIG	0 063				
		--	--	--	41	MIG	0 125				
		--	--	-	37	MIG	0 188				
		--	--	--	45	MIG	0 200				
		--	--	-	39	MIG	0 250				
7Al-1Mo-1V	T-88	122 5	1478	76	66	MIG	℄	1	1 2	1 32	
		--	-	72	61	MIG	3 16				
		--	612	100	82	MIG	℄				1800 F 1 hr He cool
		--	--	97	92	MIG	3 16				
5Al-2V-2Mo-2Sn	T-90	116 9	651	80	75	MIG	℄	1	1 2	1 32	
		--	--	66	47	MIG	3 16				
		--	612	103	87	MIG	℄				1660 F 1 hr He cool
		--	--	120	95	MIG	3 16				
6Al-4V	T-91	116 0	1173	83	74	MIG	℄	1	1 2	1 32	
		--	--	115	94	MIG	3 16				
6Al-6V-2Sn-1Cu-1 2Fe	T-92	137 3	--	52	49	MIG	℄	1	1 2	1 32	
		--	--	68	48	MIG	3 16				
		--	455	80	66	MIG	℄				1660 F 1 hr He cool
		--	--	106	74	MIG	3 16				
6Al-3V-1Mo	T-93	113 8	--	102	95	MIG	℄	1	1 2	1 32	
		--	--	106	90	MIG	3 16				
			1173	104	84	MIG	℄				1650 F 1 hr He cool
		--	--	110	92	MIG	3 16				
7Al 2 1 2Mo	T-94	111 9	--	66	59	MIG	℄	1	1 2	1 32	
		-	--	92	5[illegible]	MIG	3 16				
		--	931	90†	74†	MIG	℄				1800 F 1 hr He cool
		--	--	9[illegible]	81	MIG	3 16				
6Al-4V -0 12% O_2	T-95	-	1784	86	[illegible]5	MIG	℄	1	1 2	1 32	
		--	--	78	76	MIG	3 16				
		--	1052	106	90	MIG	℄				1850 F 1 hr He cool
		--	-	110	[illegible]4	MIG	3 16				
6Al 2Cb-1Ta-0 8Mo	T-96	--	2026	[illegible]	90	MIG	℄	1	1 2	1 32	
		-	-	100	78	MIG	1 8				
		--	--	92	77	MIG	3 16				

*MIG – Metal Inert-Gas EB – Electron Beam
†Flaws in specimens

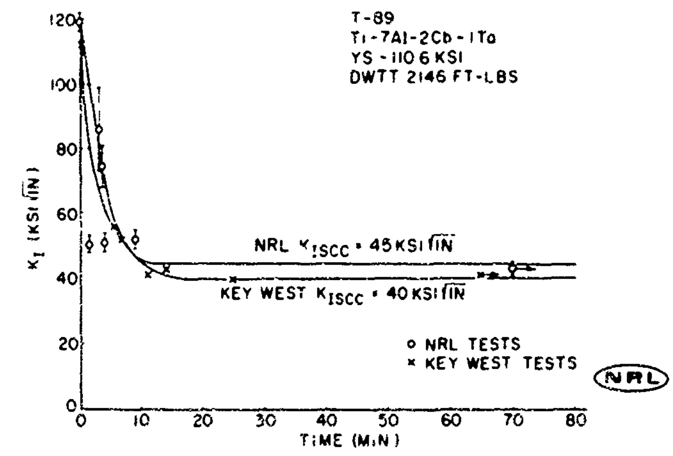

Fig. 5 - Comparison of SCC characterizations for laboratory tests in 3.5% salt water solution and in flowing sea water

DISCUSSION

The SCC data presented here do not show any direct correlation with mechanical properties, such as yield strength, drop weight tear energy, and Charpy V energy. All the alloys tested showed some degree of sensitivity to SCC, though several alloys showed only a very slight susceptibility. The distribution of the data and the lack of a trend are well illustrated in the stress-corrosion cracking resistance index chart, Fig. 4.

Lacking a correlation of any kind at this time, it is difficult to predict with any degree of precision the relative degree of sensitivity to SCC of a particular alloy without conducting SCC tests. It should be noted that differing levels of K_{Iscc} were found for different heats of alloys with the same nominal composition, which indicates that processing variables play a role in determining SCC sensitivity. However, a general indication of approximate levels of sensitivity to SCC can be realized from these data if these factors are considered.

Recently it was found that a Ti-6Al-4V alloy was extremely SCC sensitive to methyl alcohol whereas the same material did not appear to be affected by aqueous environments (6). An addition of approximately 1% H_2O to the methyl alcohol provided the "fix" to this problem encountered in one of our space programs. Such experiments serve to indicate that the SCC resistance of metals being contemplated for structural design should be determined for each and every type of service and preservice environment it will see. This experience also points up the difficulty of predicting just what ingredients can be used to neutralize a normally hostile environment.

ACKNOWLEDGMENTS

The authors express their appreciation to Dr. B. F. Brown for his interest and suggestions related to this study, to Mr. R. W. Huber for providing the weldments and for his overall interest in this effort, and to the Advanced Research Projects Agency and the Deep Submergence Systems Project for their support.

REFERENCES

1. Brown, B.F., et al., "Marine Corrosion Studies (Third Interim Report of Progress)," NRL Memorandum Report 1634, July 1965

2. Brown, B.F., "A New Stress-Corrosion Cracking Test Procedure for High-Strength Alloys," Mat. Res. Std. 6: 3, (1966)

3. Kies, J.A., et al., "Fracture Testing of Weldments," In "Fracture Toughness Testing and Its Applications," Philadelphia: ASTM, pp. 328-356, 1965

4. Pellini, W.S., et al., "Review of Concepts and Status of Procedures for Fracture-Safe Design of Complex Welded Structures Involving Metals of Low to Ultra-High Strength Levels," NRL Report 6300, June 1965

5. Seeley, R.R., Seagle, S.R., and Bertea, O., "Development of a Titanium-Base Alloy for Sea Water Environments," presented at the conference on "Physical Metallurgy of Titanium," AIME Fall Meeting, Oct. 30-Nov. 3, 1966, Chicago, Illinois. Also Reactive Metals, Inc. Research Report R480, Nov. 2, 1966

6. Brown, B.F., private communication

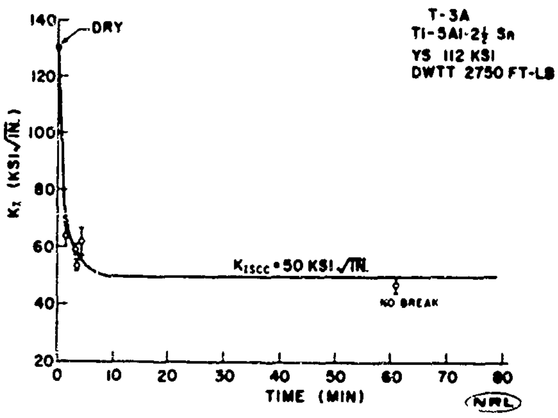

Fig. 6 - Environmental cracking characterization curve for titanium alloy T-3

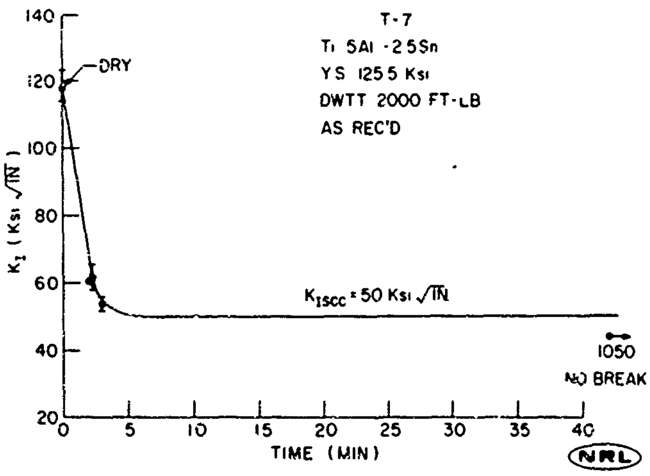

Fig. 7 - Environmental cracking characterization curve for titanium alloy T-7

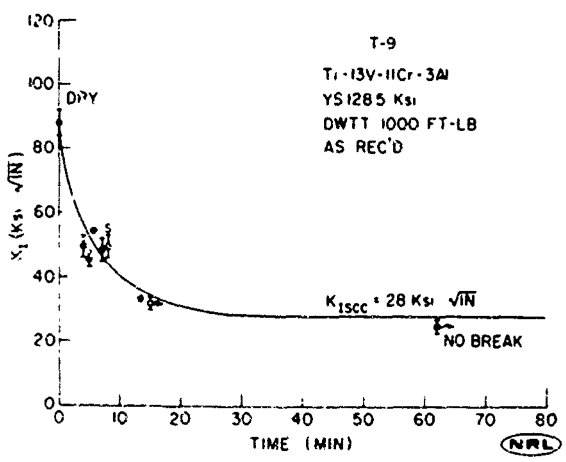

Fig. 8 - Environmental cracking characterization curve for titanium alloy T-9

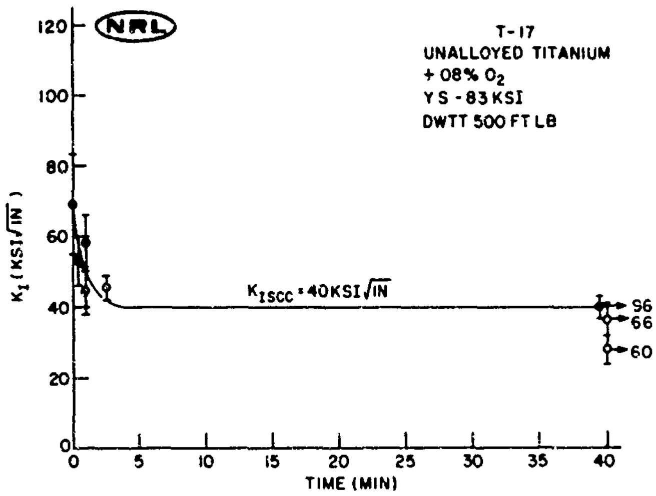

Fig. 9 - Environmental cracking characterization curve for titanium alloy T-17

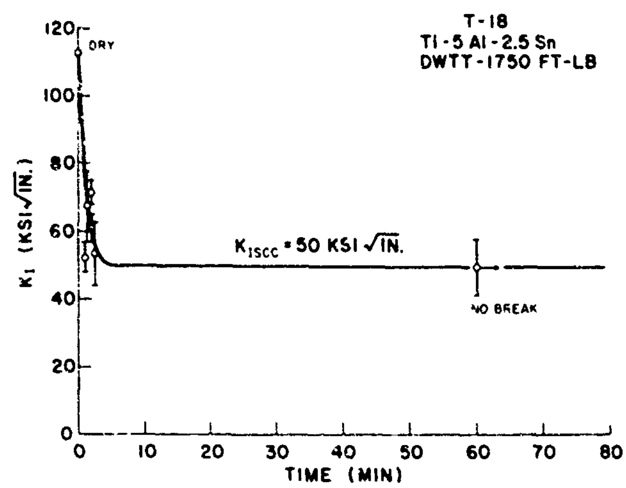

Fig. 10 - Environmental cracking characterization curve for titanium alloy T-18

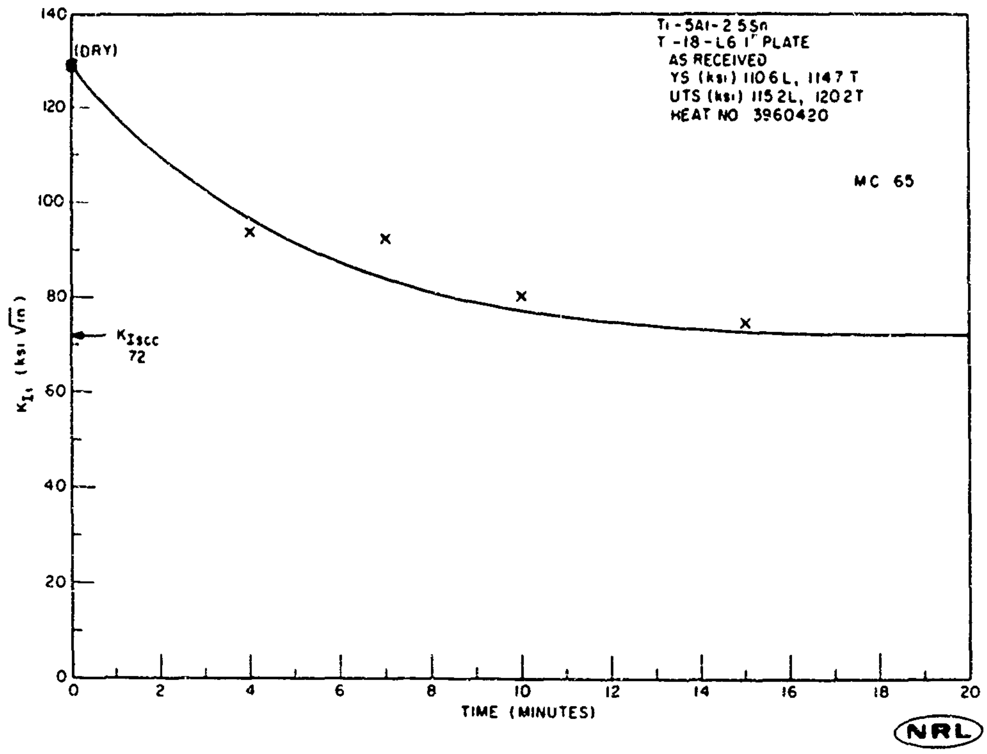

Fig. 11 - Environmental cracking characterization curve for titanium alloy T-18

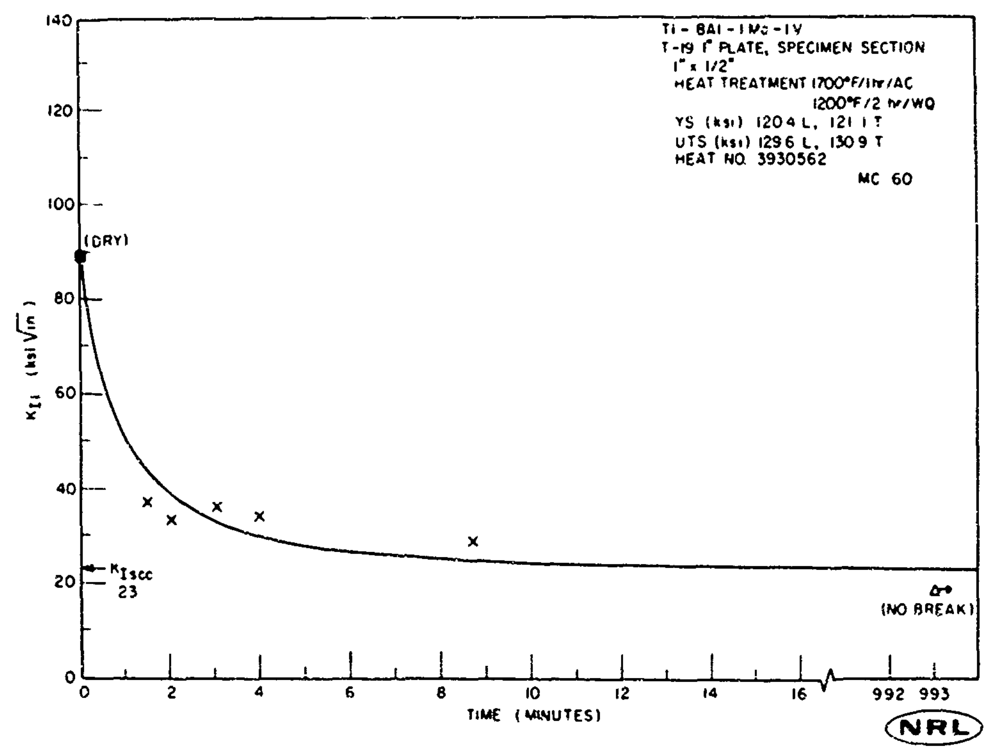

Fig. 12 - Environmental cracking characterization curve for titanium alloy T-19

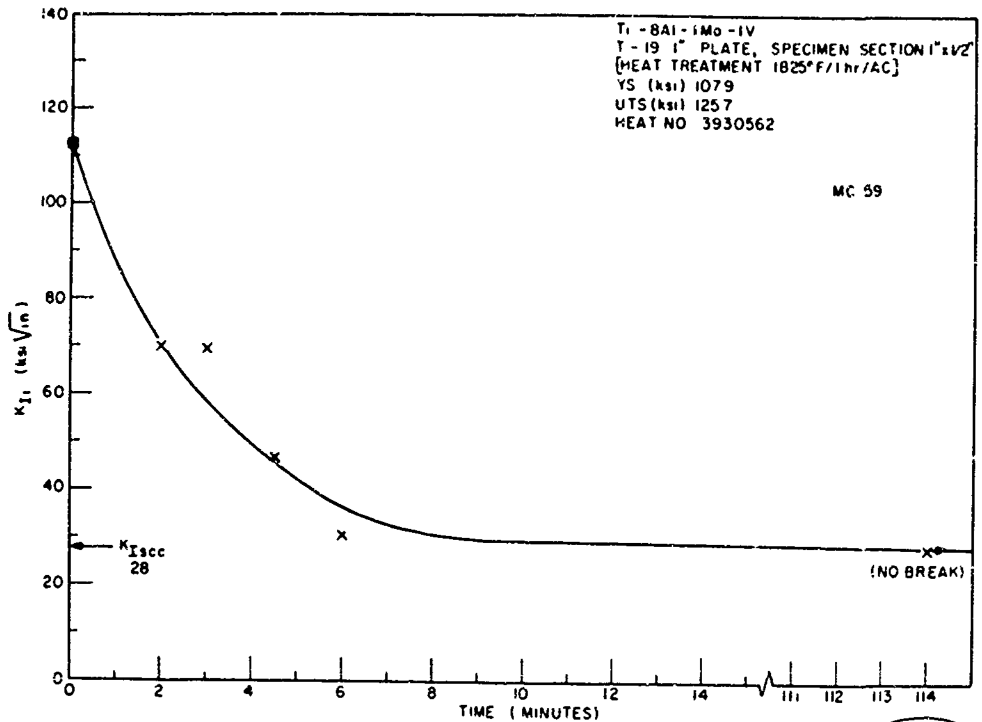

Fig. 13 - Environmental cracking characterization curve for titanium alloy T-19

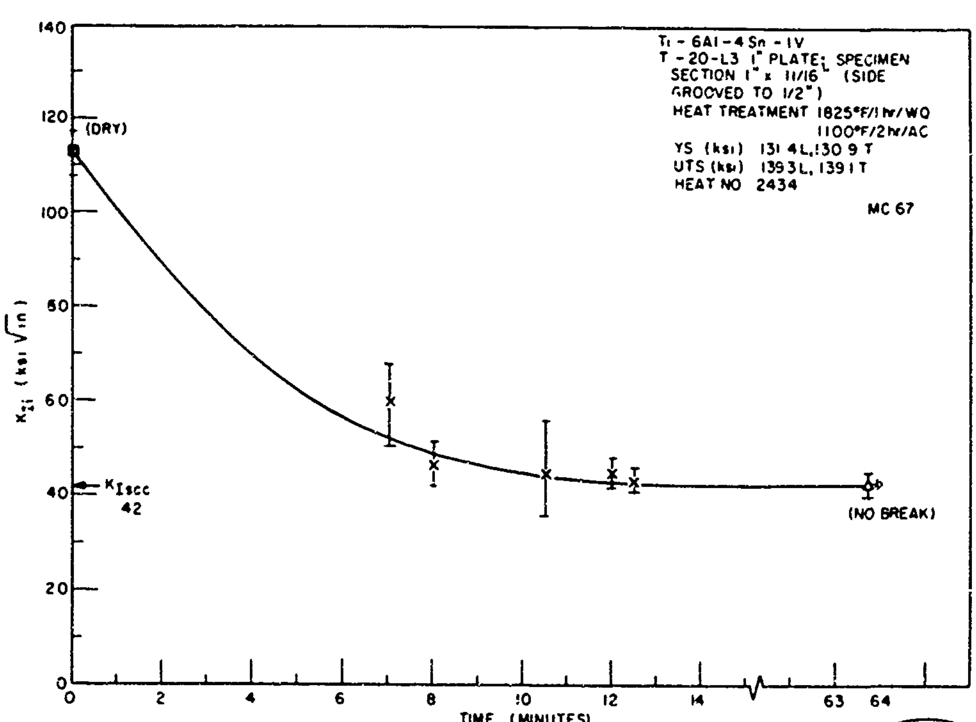

Fig. 14 - Environmental cracking characterization curve for titanium alloy T-20

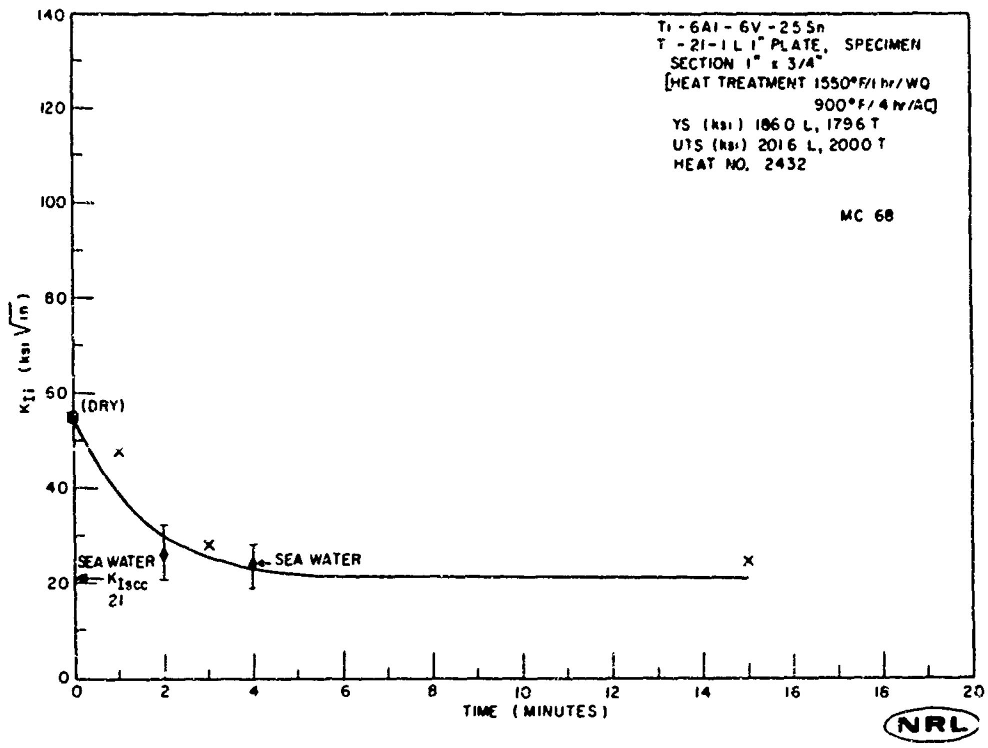

Fig. 15 - Environmental cracking characterization curve for titanium alloy T-21

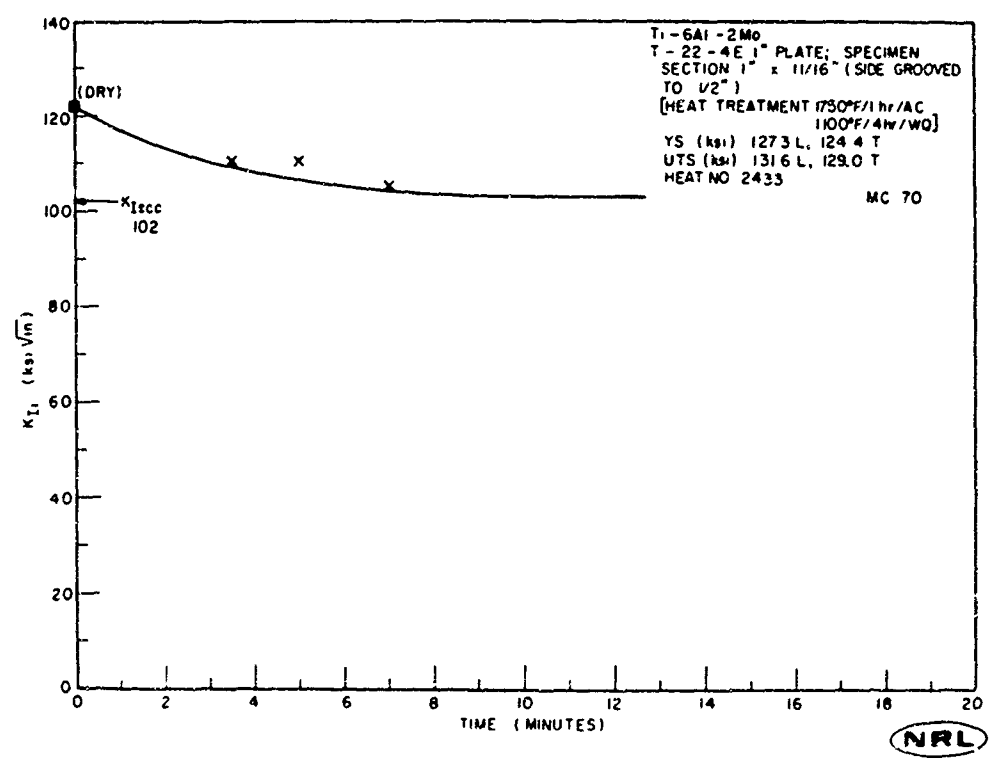

Fig. 16 - Environmental cracking characterization curve for titanium alloy T-22

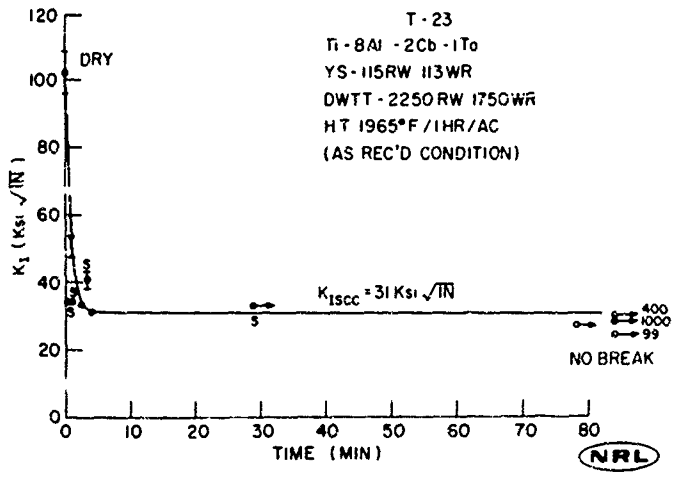

Fig. 17 - Environmental cracking characterization curve for titanium alloy T-23

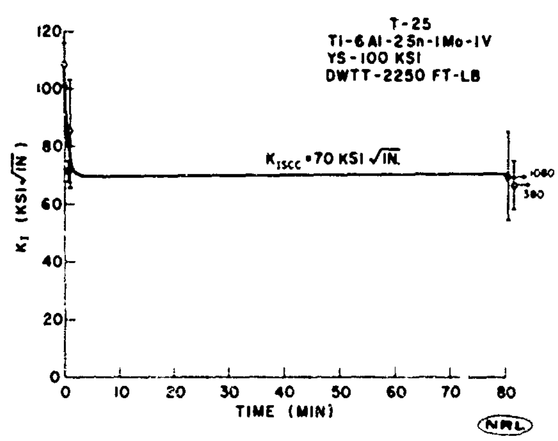

Fig. 18 - Environmental cracking characterization curve for titanium alloy T-25

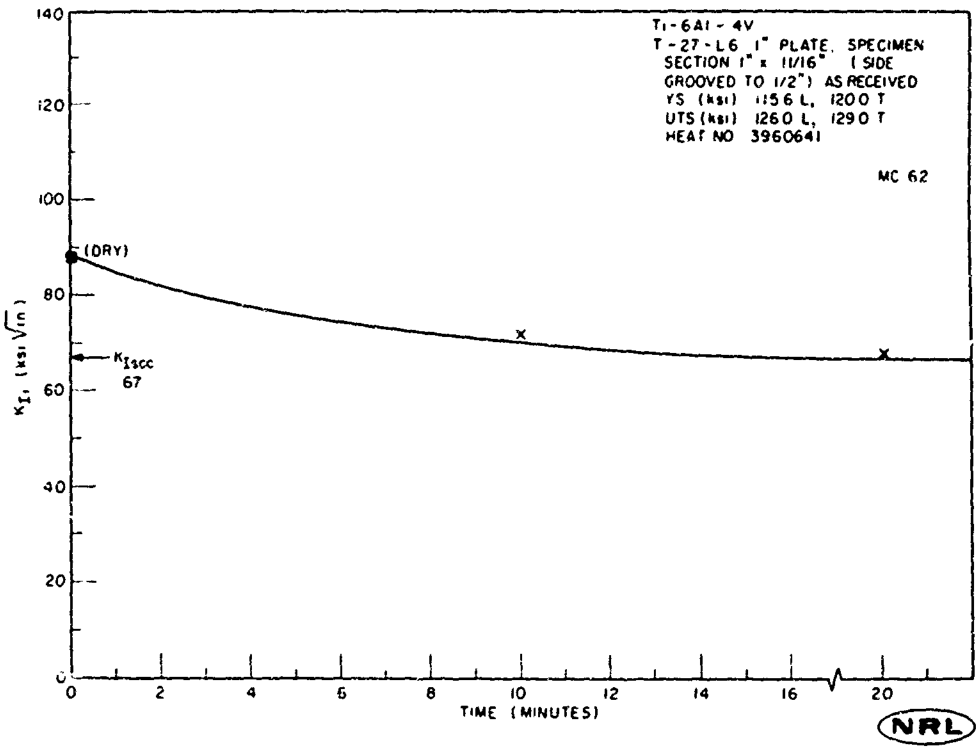

Fig. 19 - Environmental cracking characterization curve for titanium alloy T-27

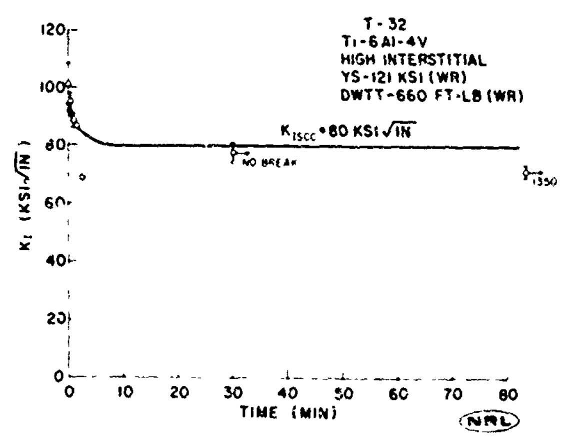

Fig. 20 - Environmental cracking characterization curve for titanium alloy T-32

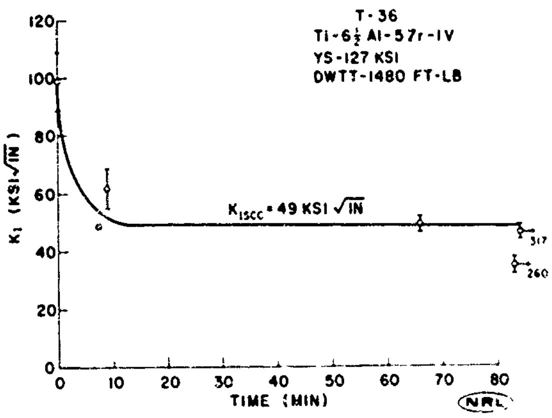

Fig. 21 - Environmental cracking characterization curve for titanium alloy T-36

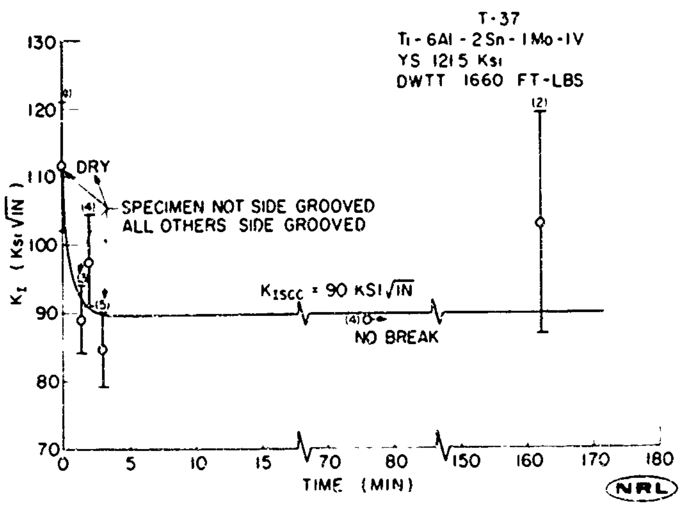

Fig. 22 - Environmental cracking characterization curve for titanium alloy T-37

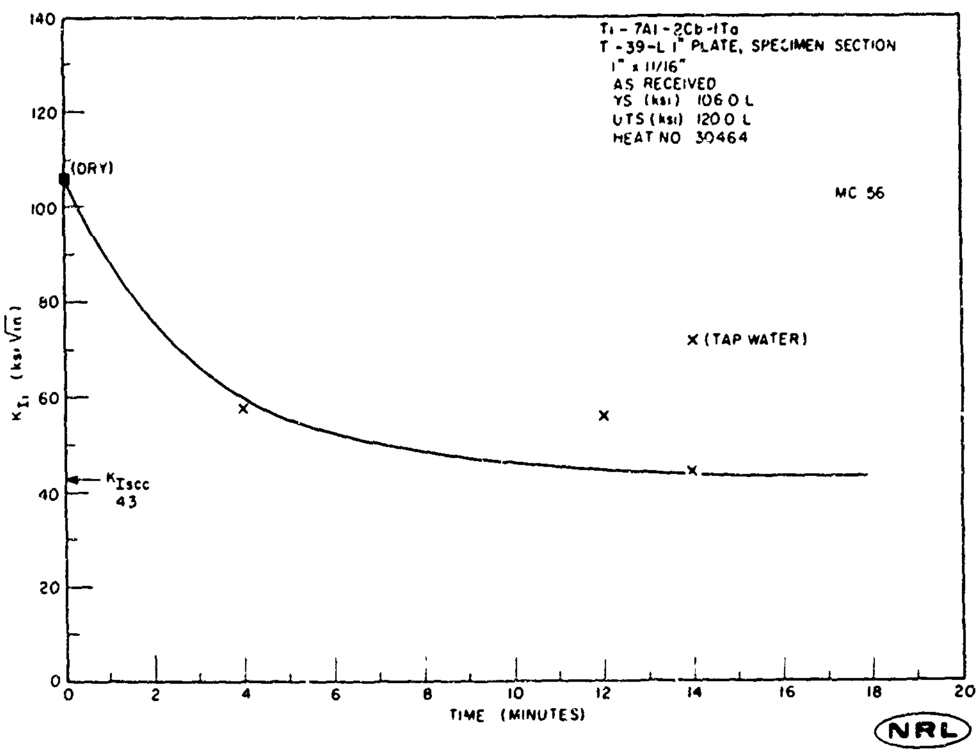

Fig. 23 - Environmental cracking characterization curve for titanium alloy T-39

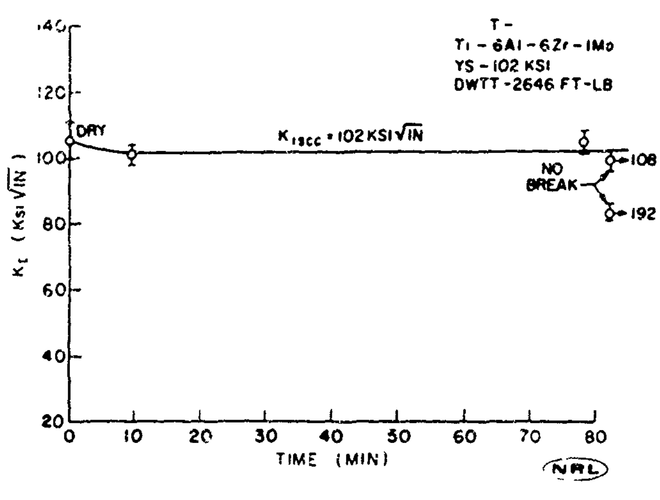

Fig. 24 - Environmental cracking characterization curve for titanium alloy T-41

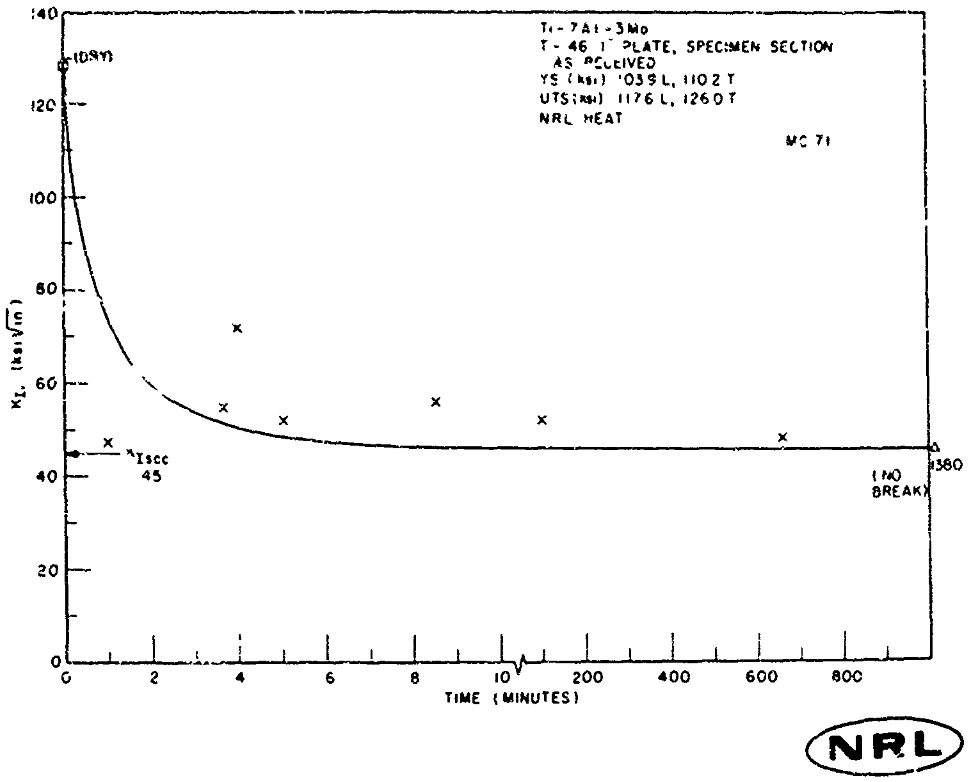

Fig. 25 - Environmental cracking characterization curve for titanium alloy T-46

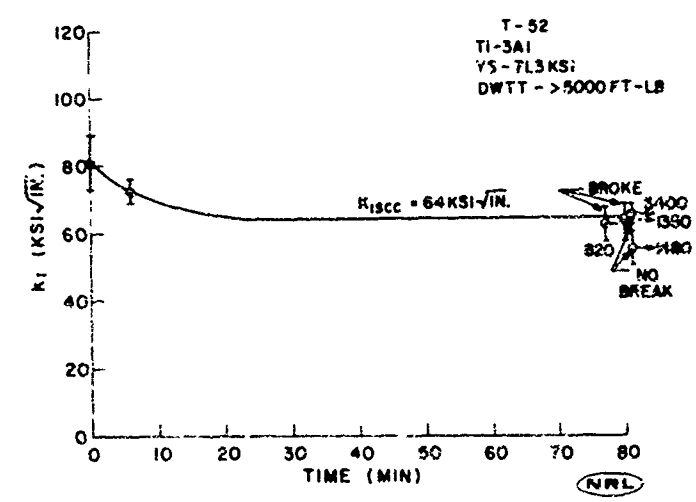

Fig. 26 - Environmental cracking characterization curve for titanium alloy T-52

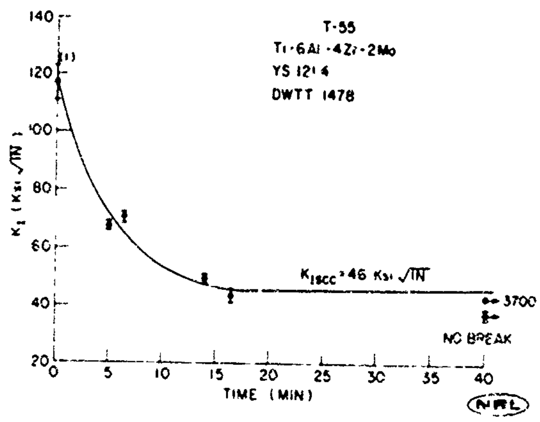

Fig. 27 - Environmental cracking characterization curve for titanium alloy T-55

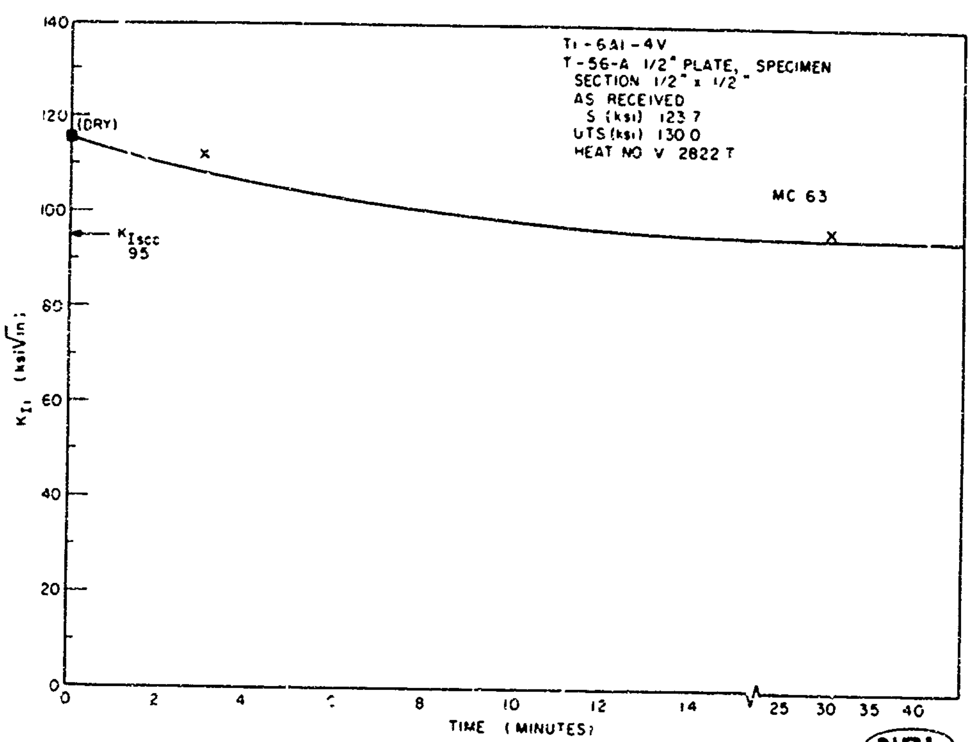

Fig. 28 - Environmental cracking characterization curve for titanium alloy T-56

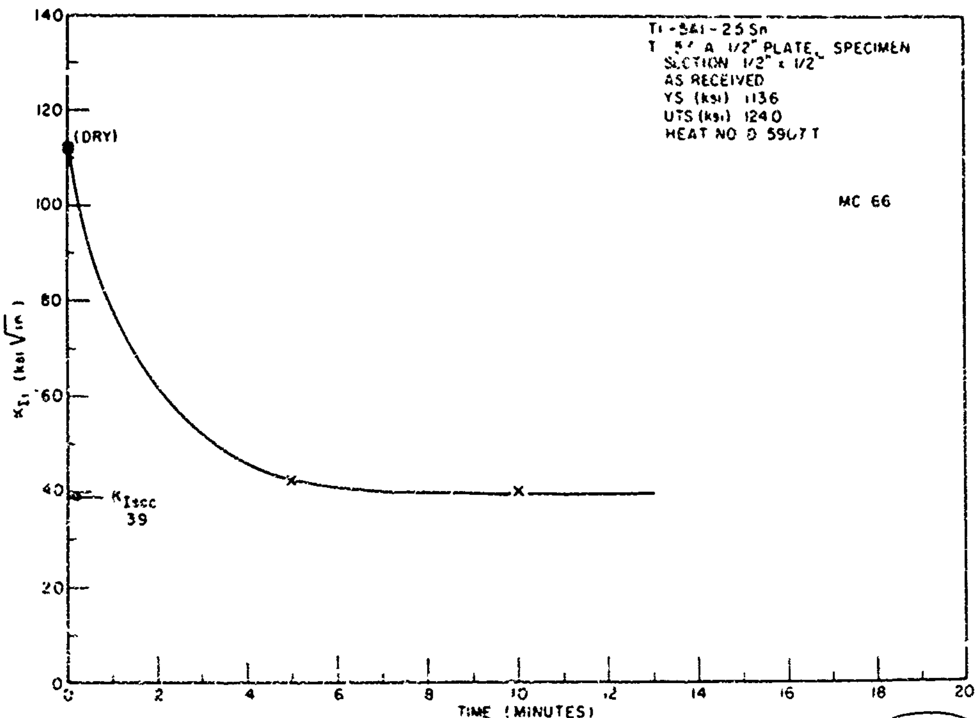

Fig. 29 - Environmental cracking characterization curve for titanium alloy T-57

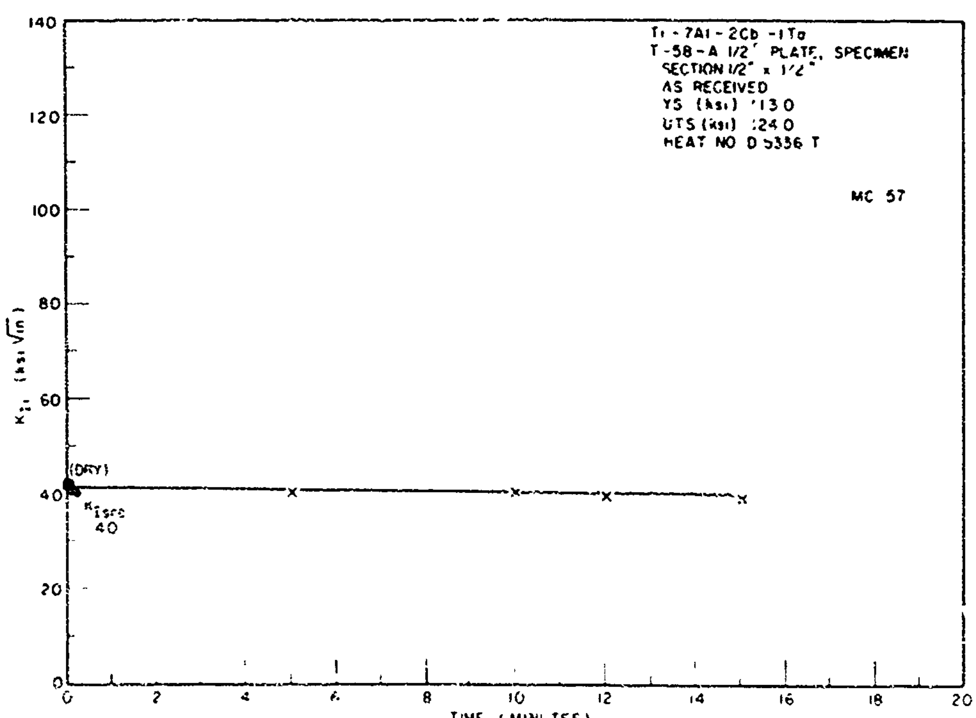

Fig. 30 - Environmental cracking characterization curve for titanium alloy T-58

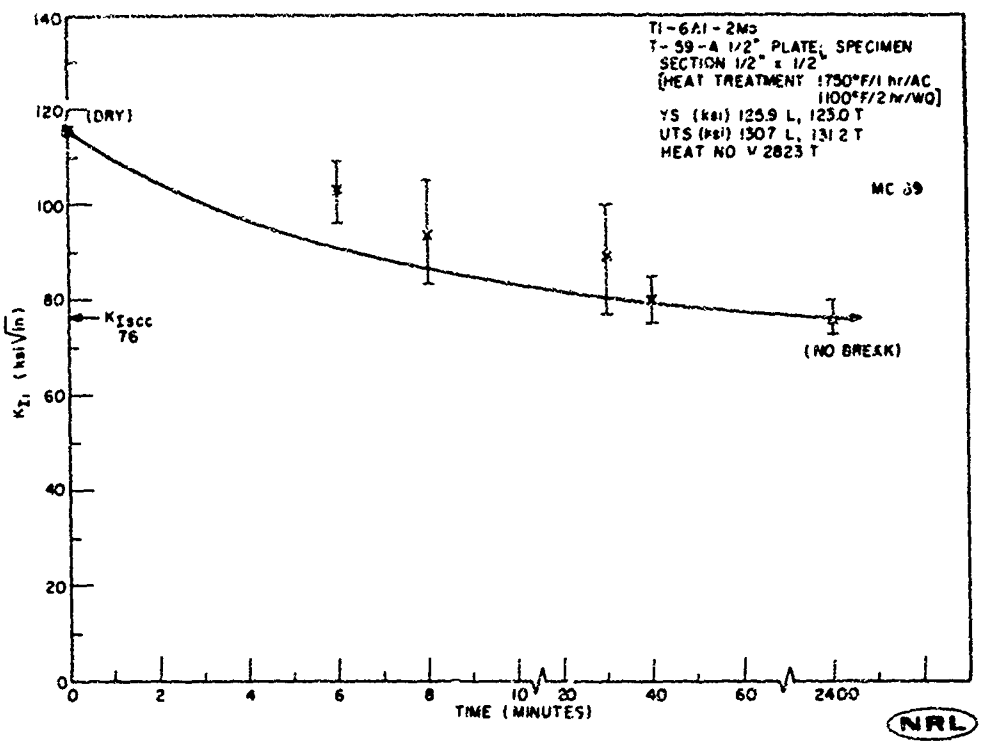

Fig. 31 - Environmental cracking characterization curve for titanium alloy T-59

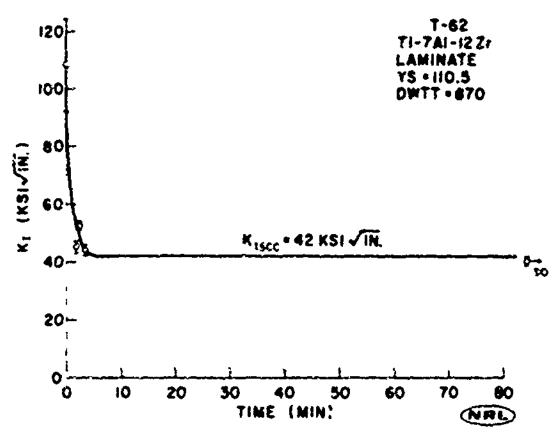

Fig. 32 - Environmental cracking characterization curve for titanium alloy T-62

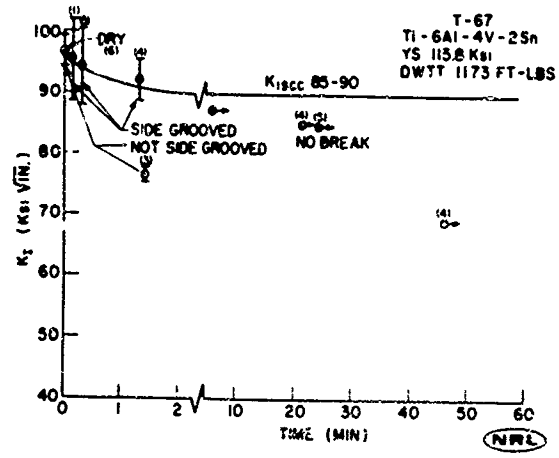

Fig. 33 - Environmental cracking characterization curve for titanium alloy T-67

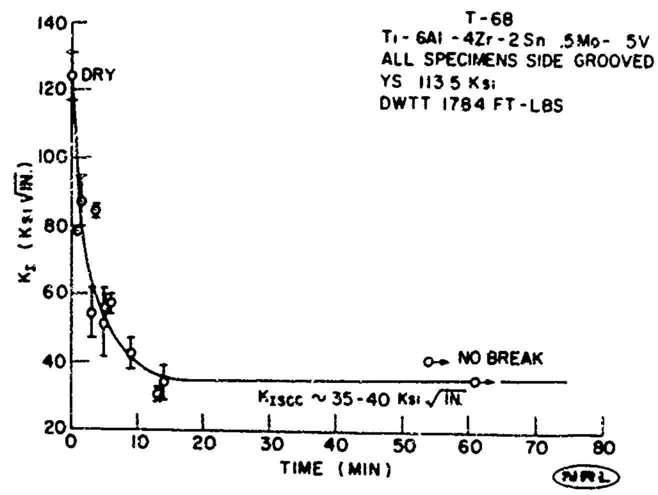

Fig. 34 - Environmental cracking characterization curve for titanium alloy T-68

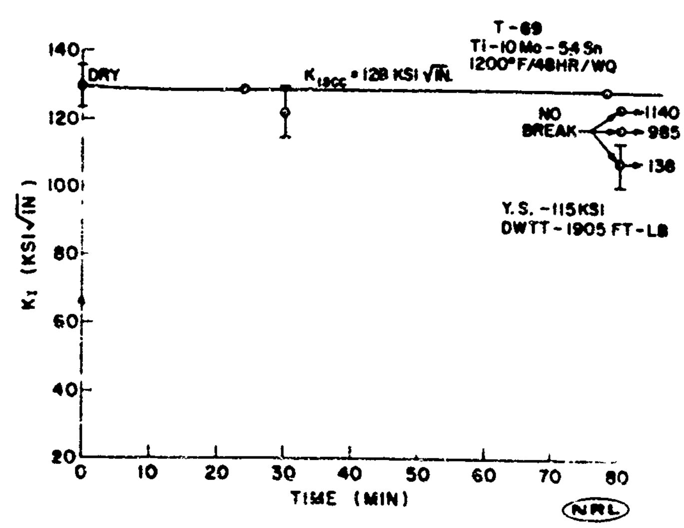

Fig. 35 - Environmental cracking characterization curve for titanium alloy T-69

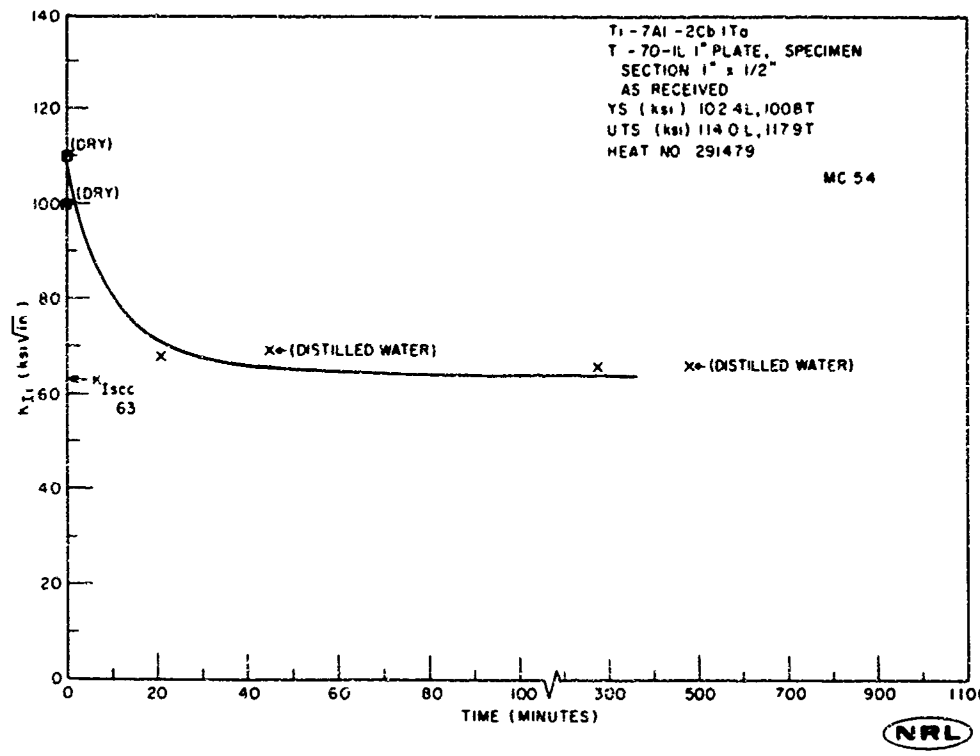

Fig. 36 - Environmental cracking characterization curve for titanium alloy T-70

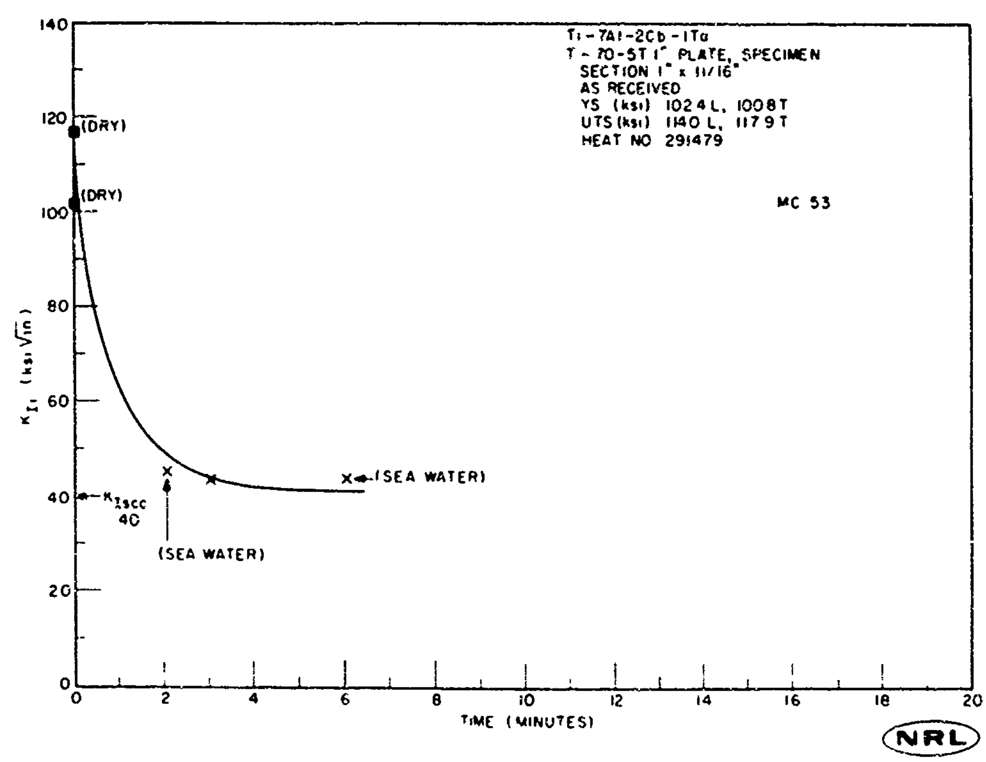

Fig. 37 - Environmental cracking characterization curve for titanium alloy T-70

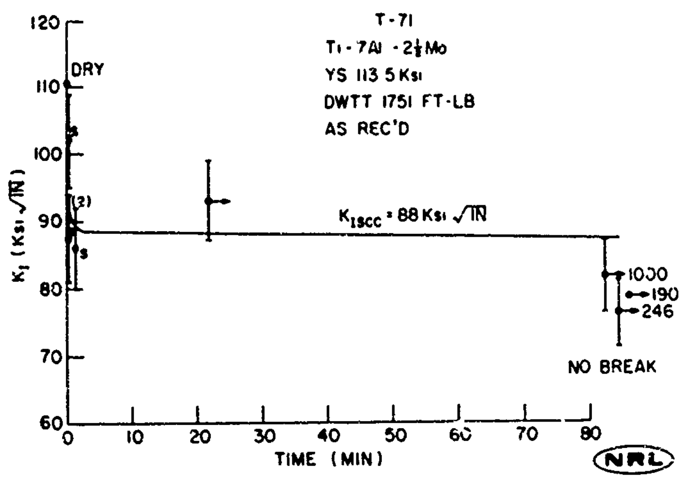

Fig. 38 - Environmental cracking characterization curve for titanium alloy T-71

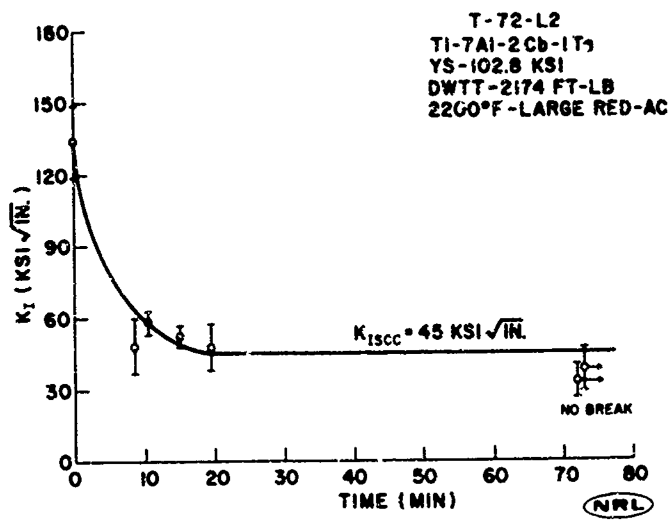

Fig. 39 - Environmental cracking characterization curve for titanium alloy T-72

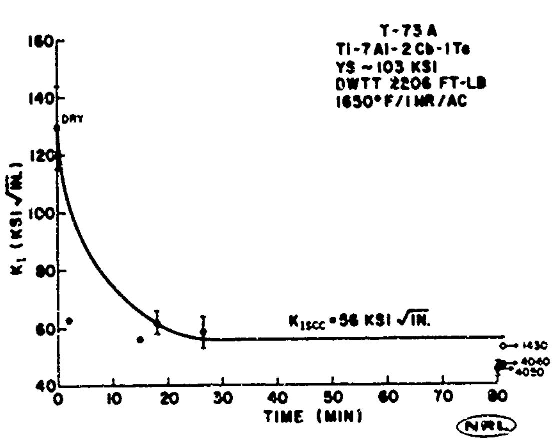

Fig. 40 - Environmental cracking characterization curve for titanium alloy T-73

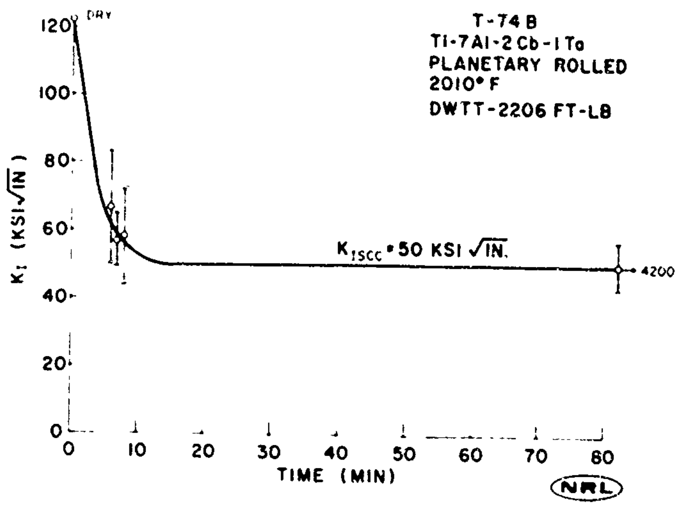

Fig. 41 - Environmental cracking characterization curve for titanium alloy T-74

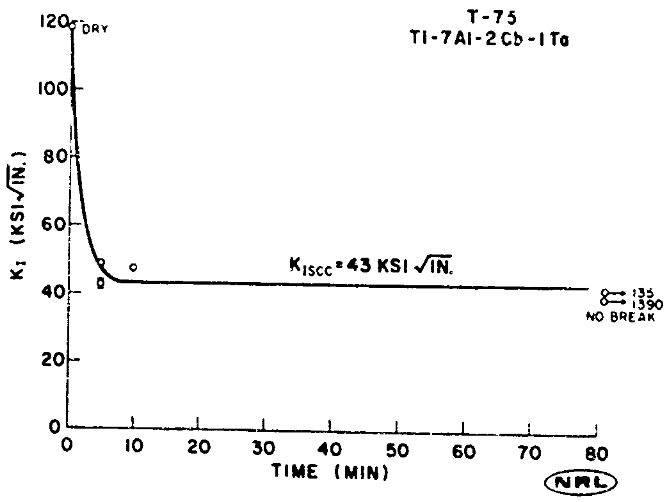

Fig. 42 - Environmental cracking characterization curve for titanium alloy T-75

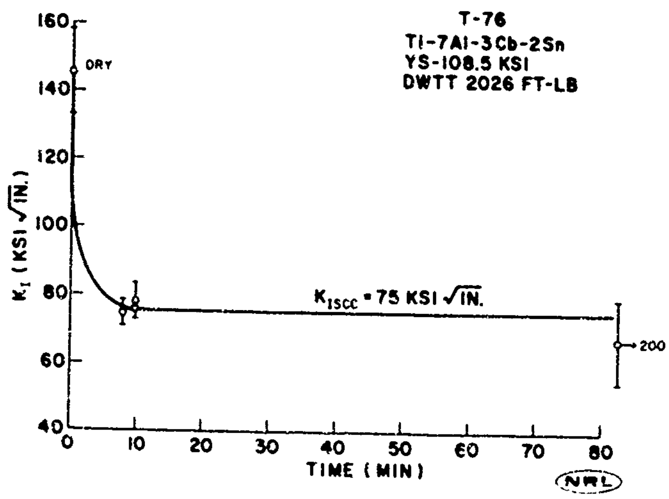

Fig. 43 - Environmental cracking characterization curve for titanium alloy T-76

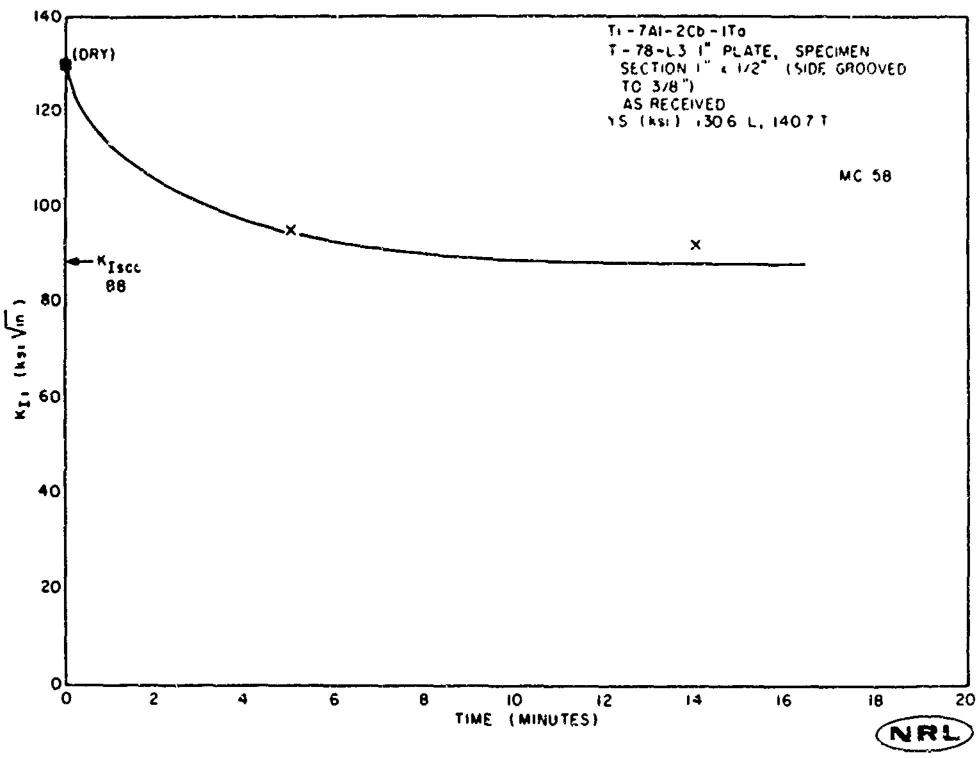

Fig. 44 - Environmental cracking characterization curve for titanium alloy T-78

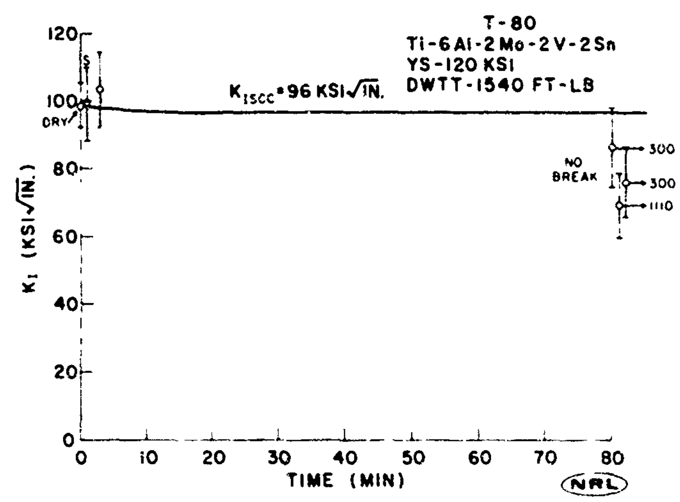

Fig. 45 - Environmental cracking characterization curve for titanium alloy T-80

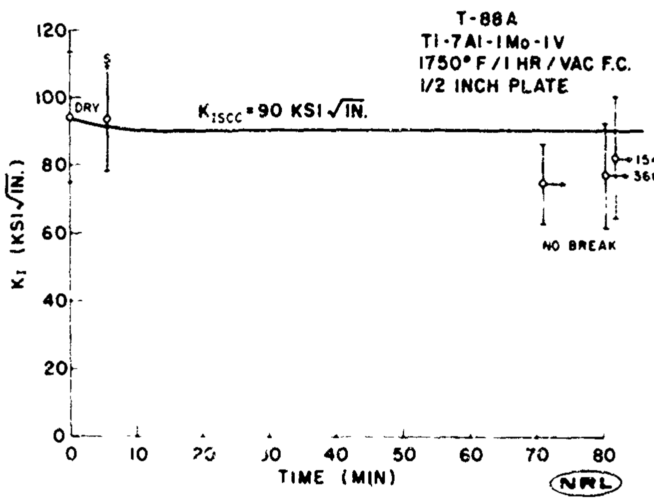

Fig. 46 - Environmental cracking characterization curve for titanium alloy T-88A

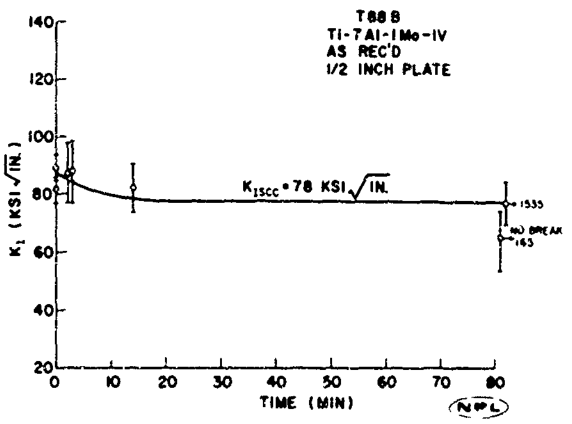

Fig. 47 - Environmental cracking characterization curve for titanium alloy T-88B

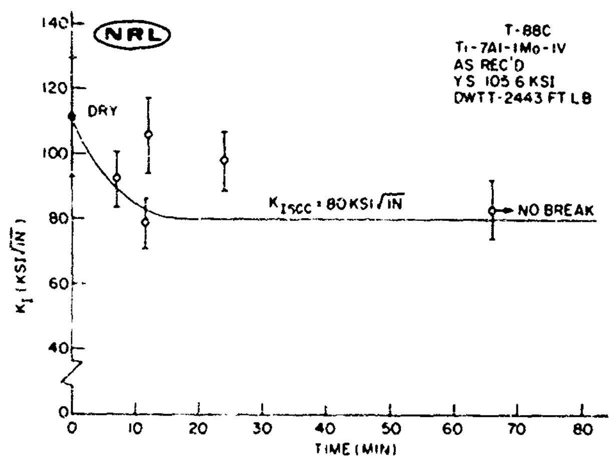

Fig. 48 - Environmental cracking characterization curve for titanium alloy T-88C

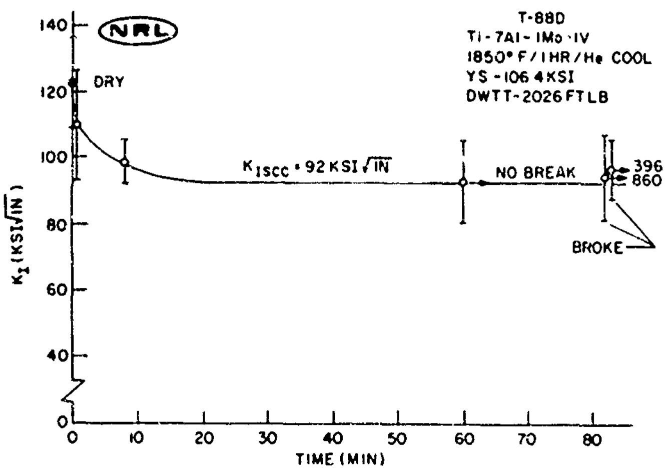

Fig. 49 - Environmental cracking characterization curve for titanium alloy T-88D

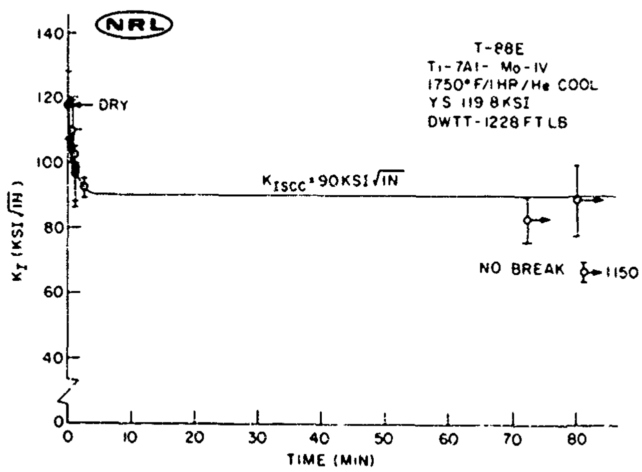

Fig. 50 - Environmental cracking characterization curve for titanium alloy T-88E

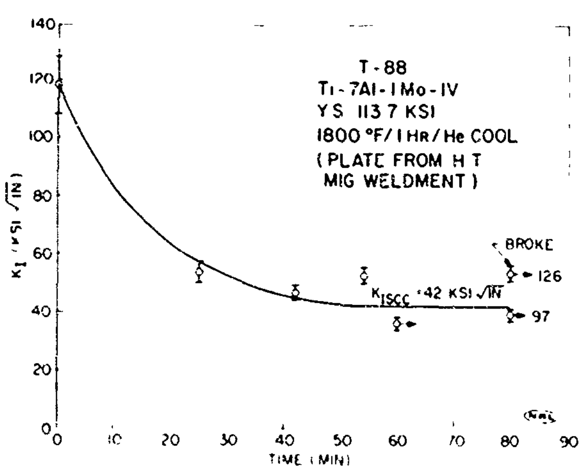

Fig. 51 - Environmental cracking characterization curve for titanium alloy T-88

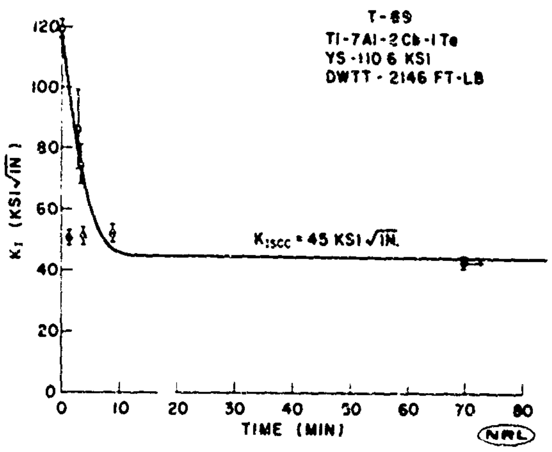

Fig. 52 - Environmental cracking characterization curve for titanium alloy T-89

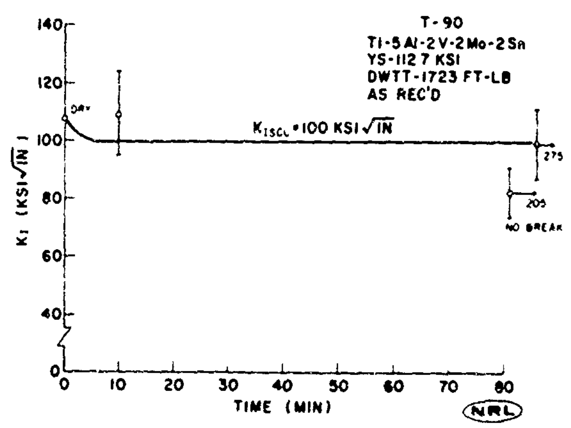

Fig. 53 - Environmental cracking characterization curve for titanium alloy T-90

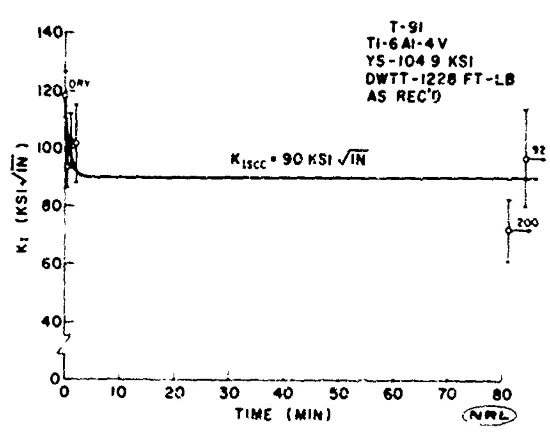

Fig. 54 - Environmental cracking characterization curve for titanium alloy T-91

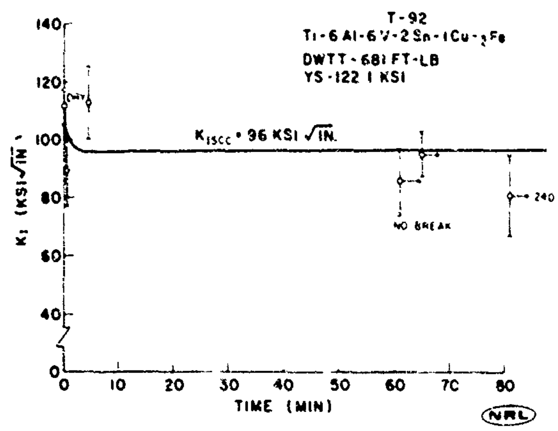

Fig. 55 - Environmental cracking characterization curve for titanium alloy T-92

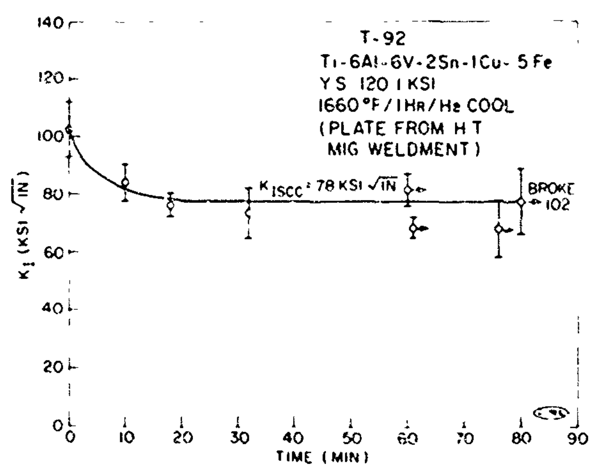

Fig. 56 - Environmental cracking characterization curve for titanium alloy T-92

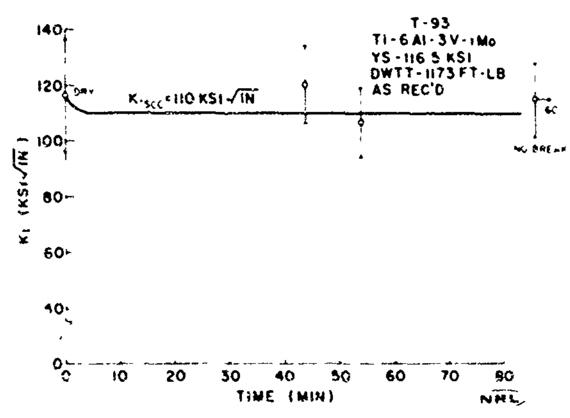

Fig. 57 - Environmental cracking characterization curve for titanium alloy T-93

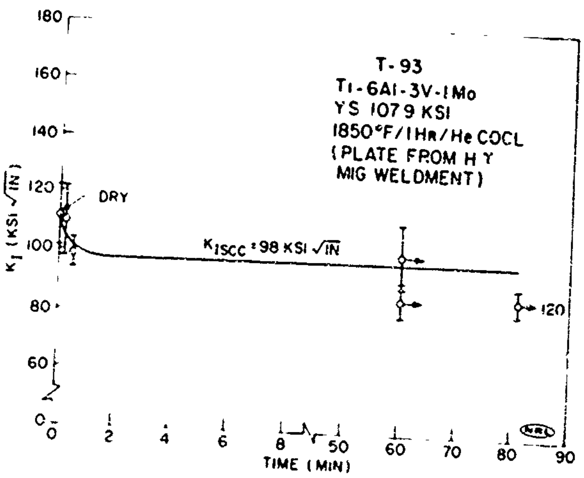

Fig. 58 - Environmental cracking characterization curve for titanium alloy T 93

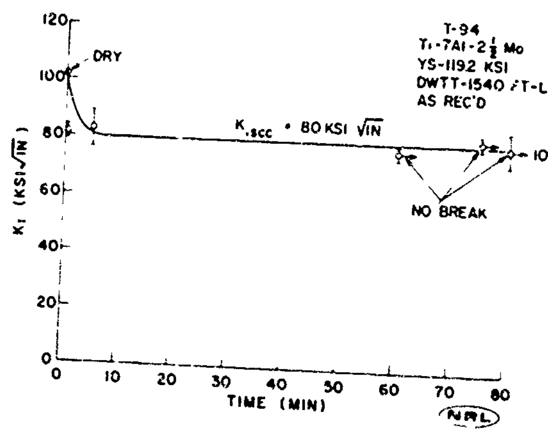

Fig. 59 - Environmental cracking characterization curve for titanium alloy T-94

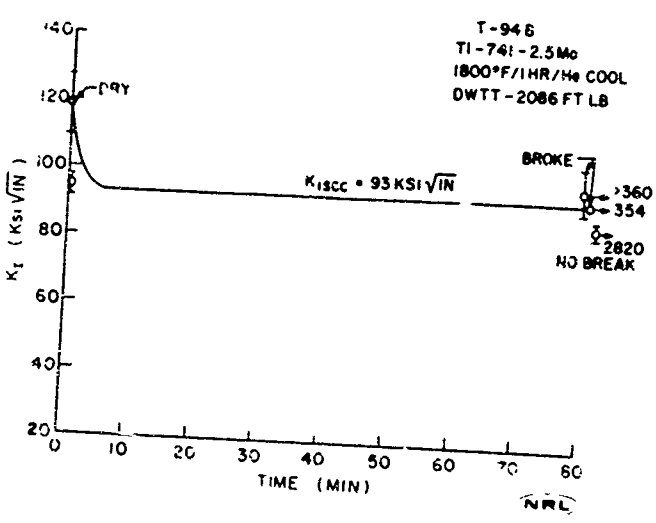

Fig. 60 - Environmental cracking characterization curve for titanium alloy T-94B

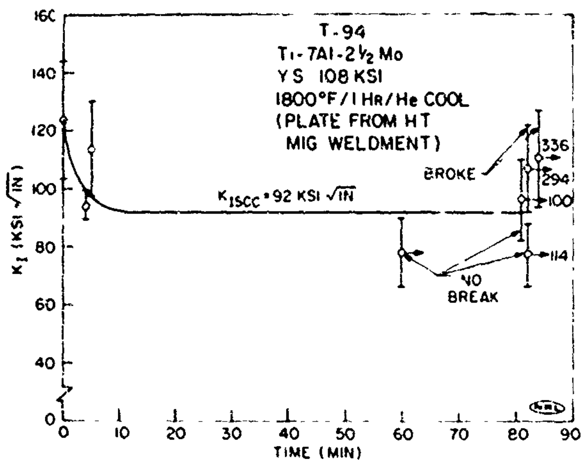

Fig. 61 - Environmental cracking characterization curve for titanium alloy T-94

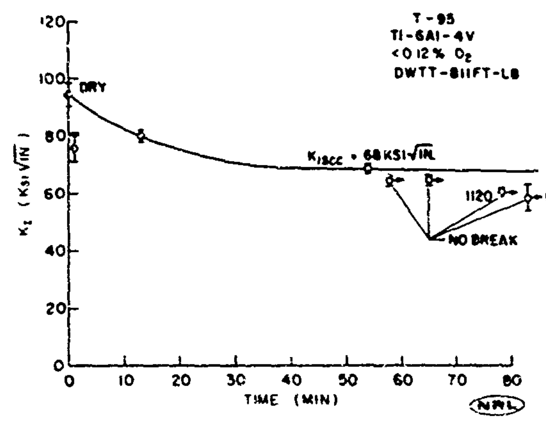

Fig. 62 - Environmental cracking characterization curve for titanium alloy T-95

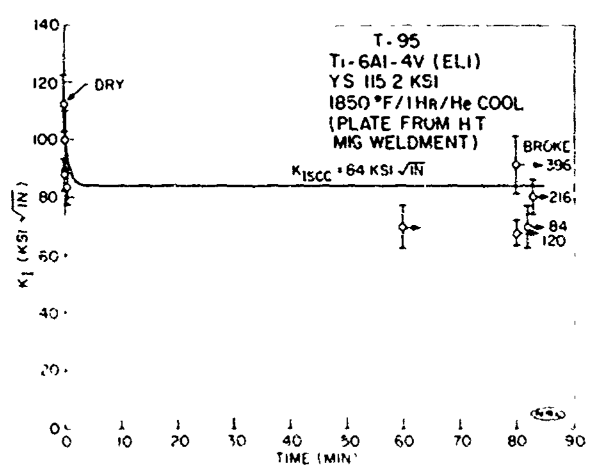

Fig. 63 - Environmental cracking characterization curve for titanium alloy T-95

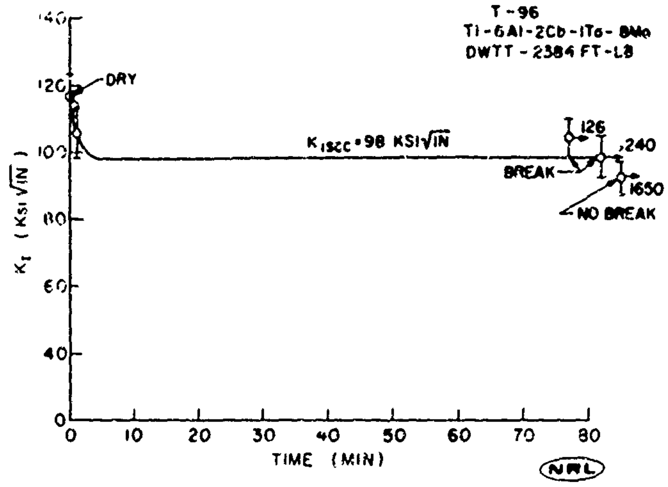

Fig. 64 - Environmental cracking characterization curve for titanium alloy T-96

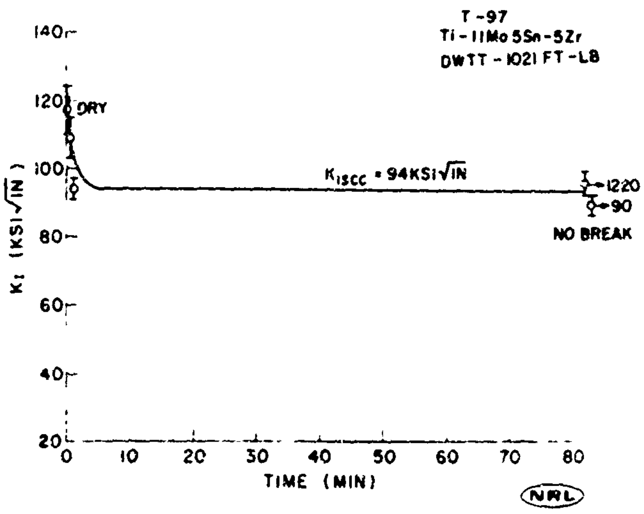

Fig. 65 - Environmental cracking characterization curve for titanium alloy T-97

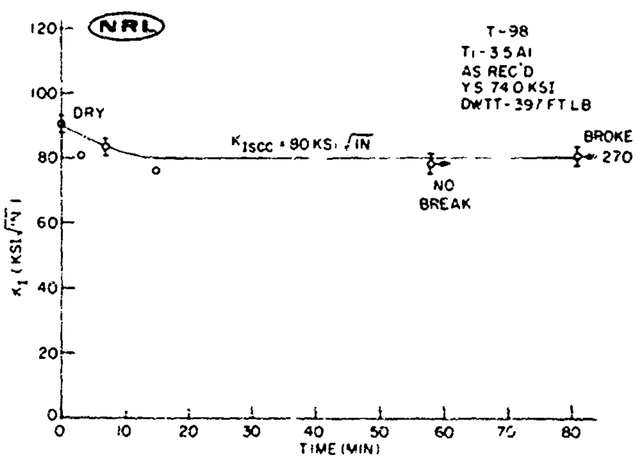

Fig. 66 - Environmental cracking characterization curve for titanium alloy T-98

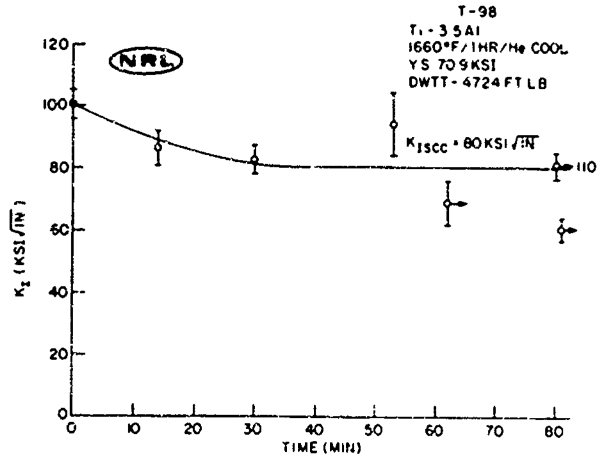

Fig. 67 - Environmental cracking characterization curve for titanium alloy T-98

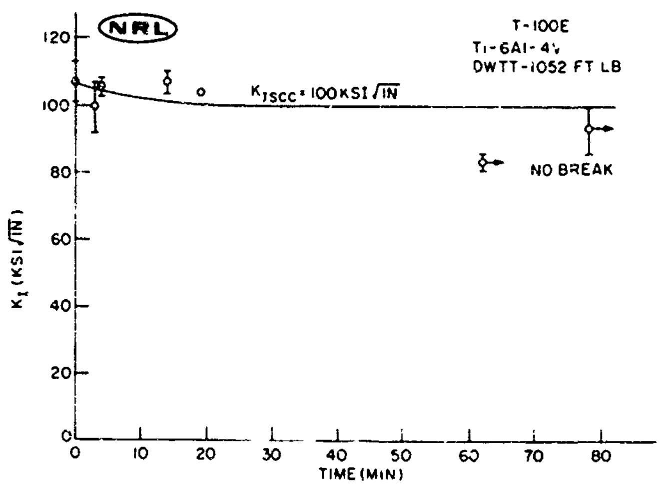

Fig. 68 - Environmental cracking characterization curve for titanium alloy T-100E

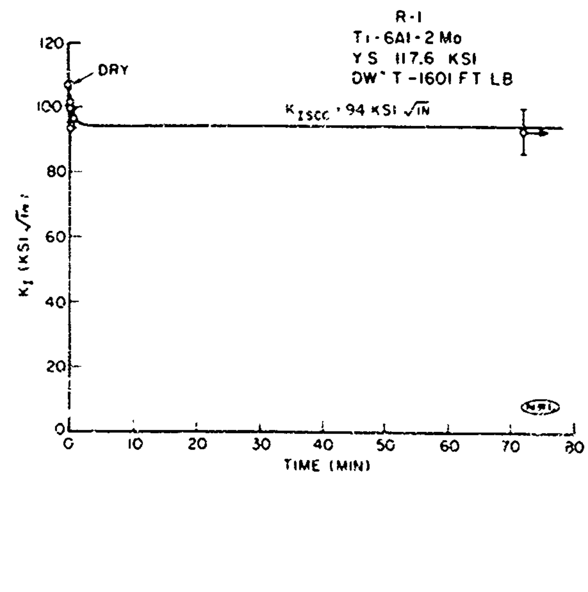

Fig. 69 - Environmental cracking characterization curve for titanium alloy R-1

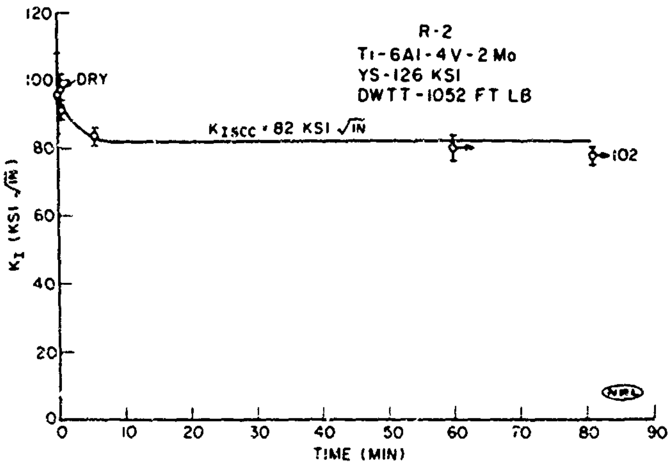

Fig. 70 - Environmental cracking characterization curve for titanium alloy R-2

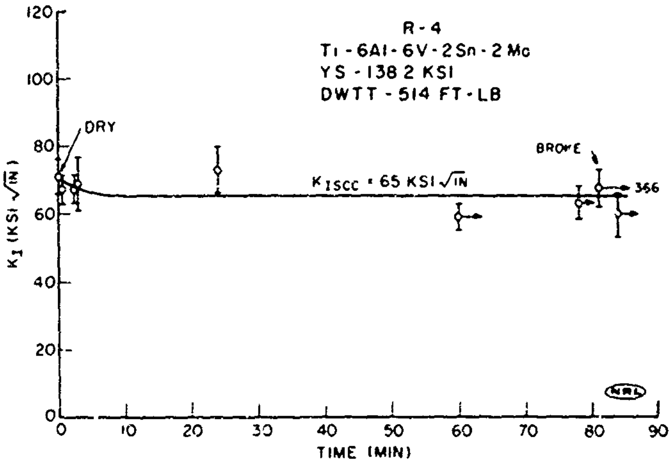

Fig. 71 - Environmental cracking characterization curve for titanium alloy R-4

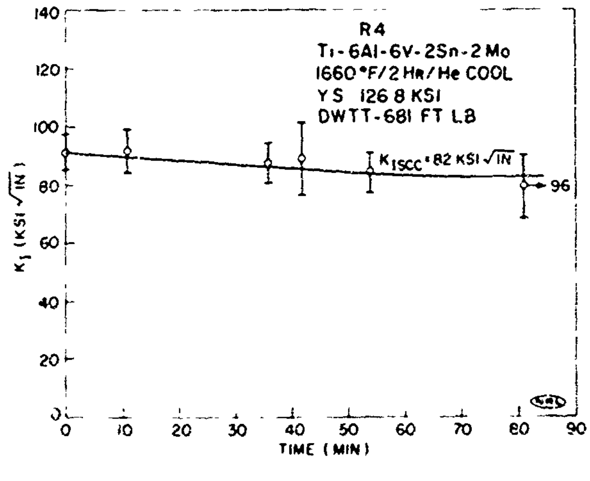

Fig. 72 - Environmental cracking characterization curve for titanium alloy R-4

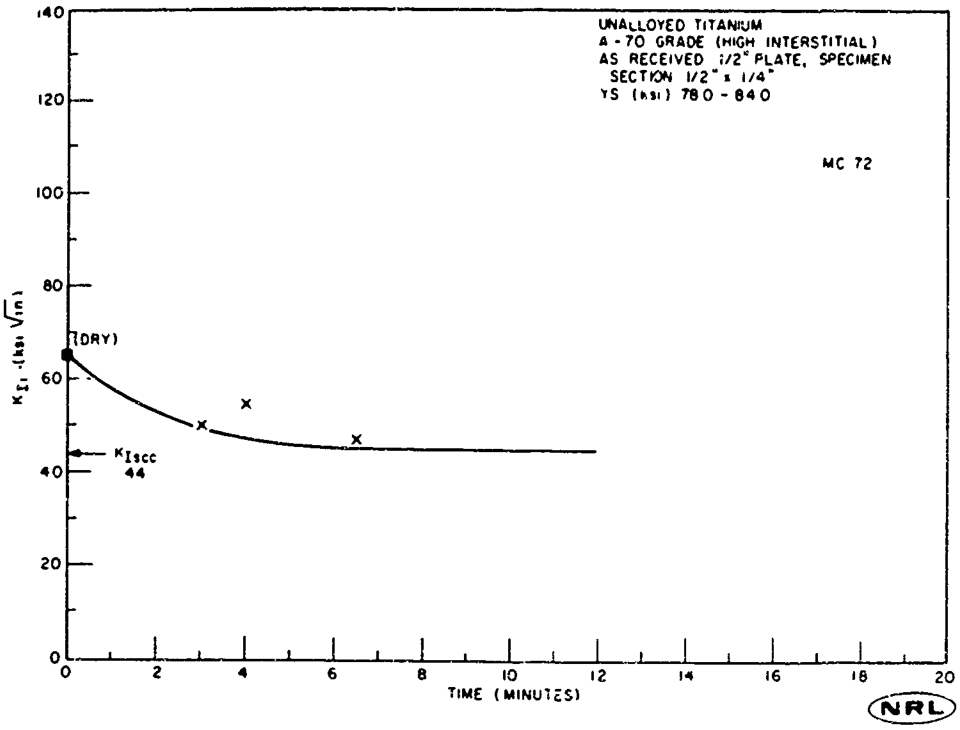

Fig. 73 - Environmental cracking characteristics of high interstitial unalloyed titanium

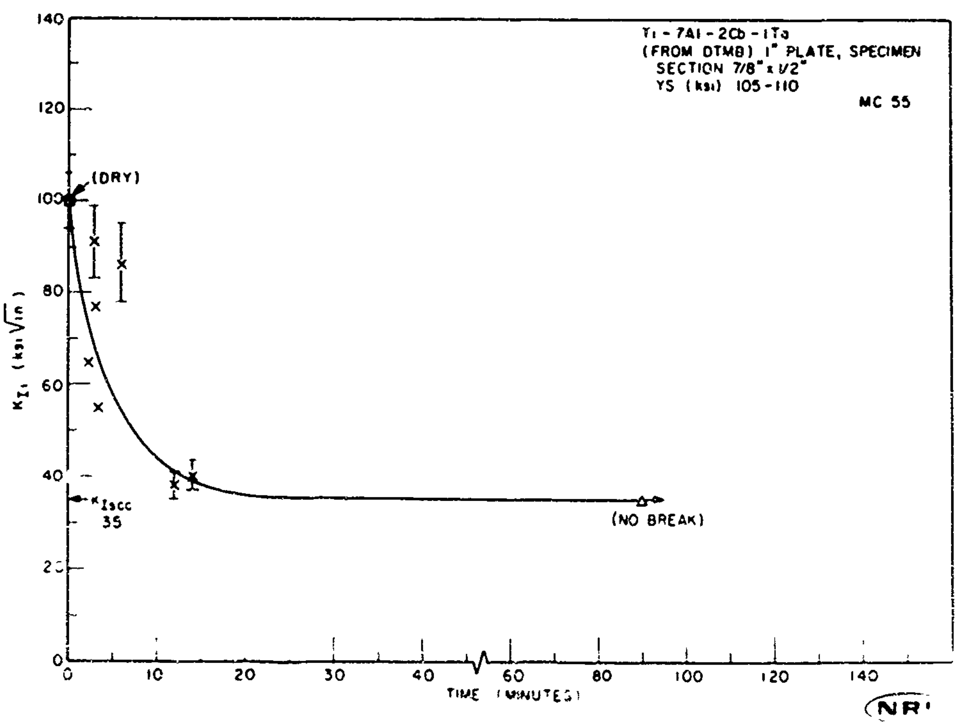

Fig. 74 - Environmental cracking characteristics of a Ti-7Al-2Cb-1Ta alloy

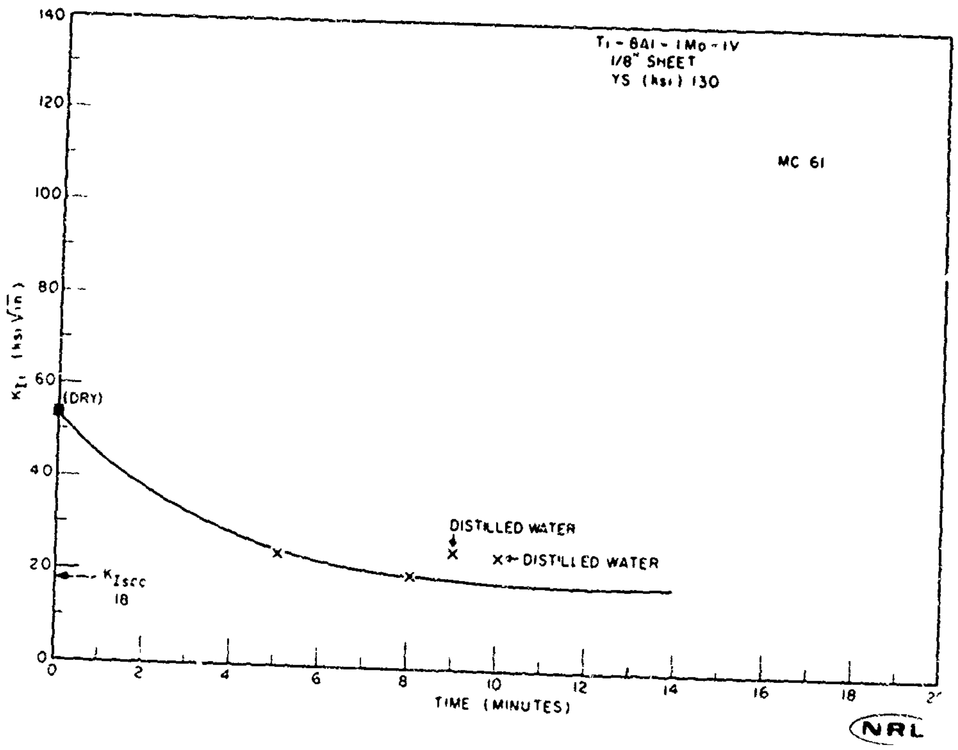

Fig. 75 - Environmental cracking characteristics of 1/8" sheet material of Ti-8Al-1Mo-1V alloy

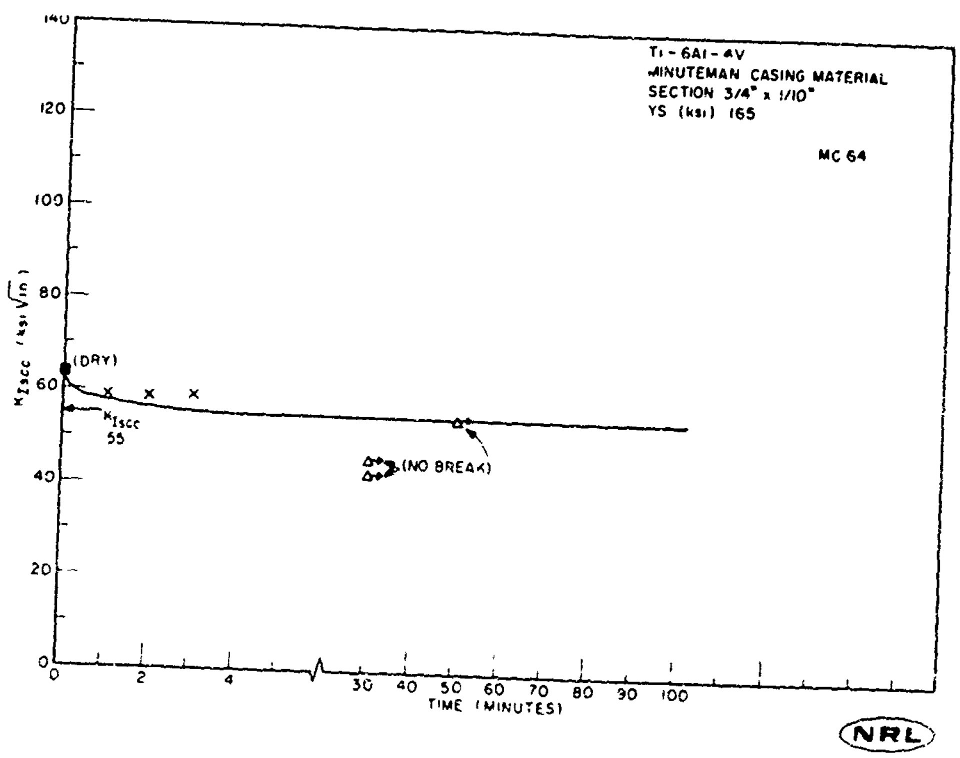

Fig. 76 - Environmental cracking characteristics of Ti-6Al-4V Minuteman casing material

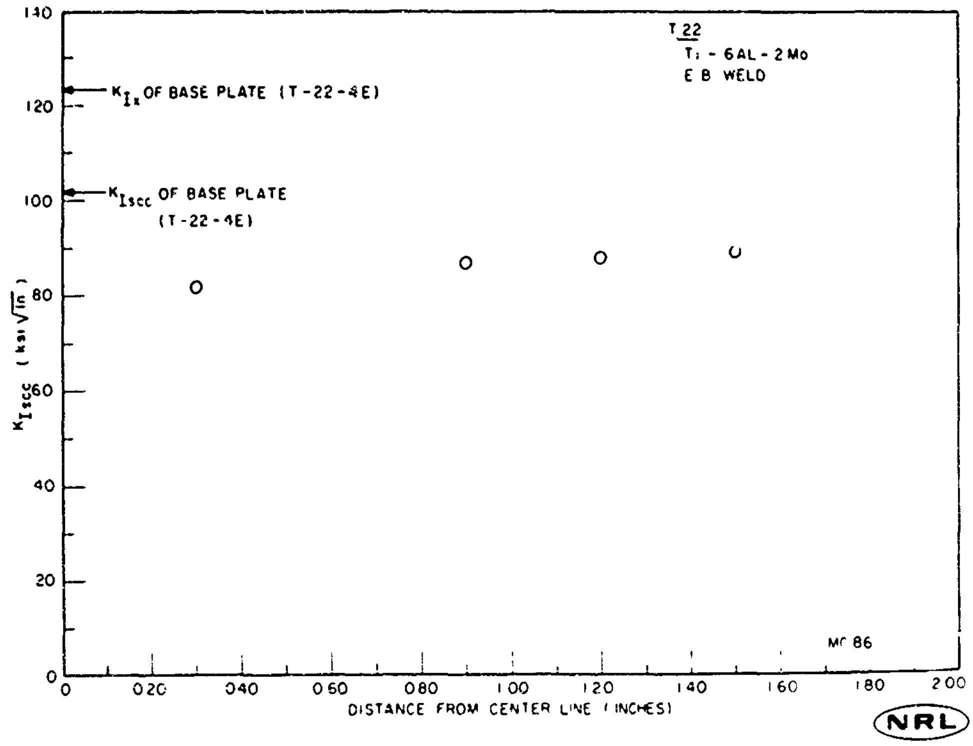

Fig. 77 - Environmental cracking characteristics of an electron beam weldment of titanium alloy T-22

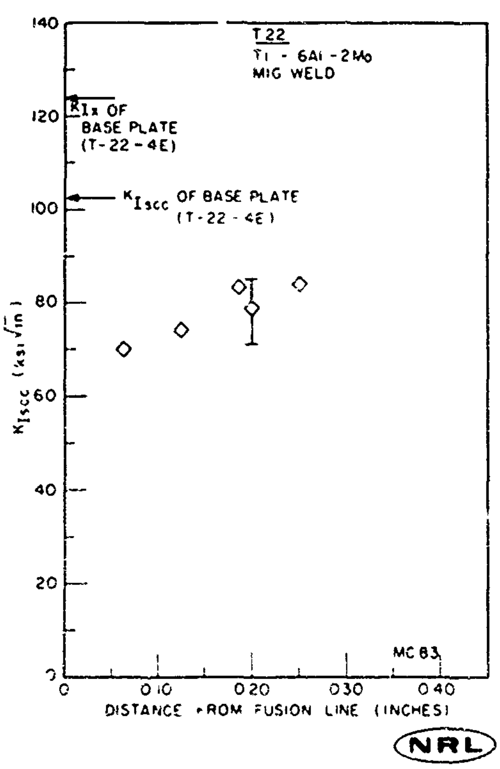

Fig. 78 - Environmental cracking characteristics of a MIG weldment of titanium alloy T-22

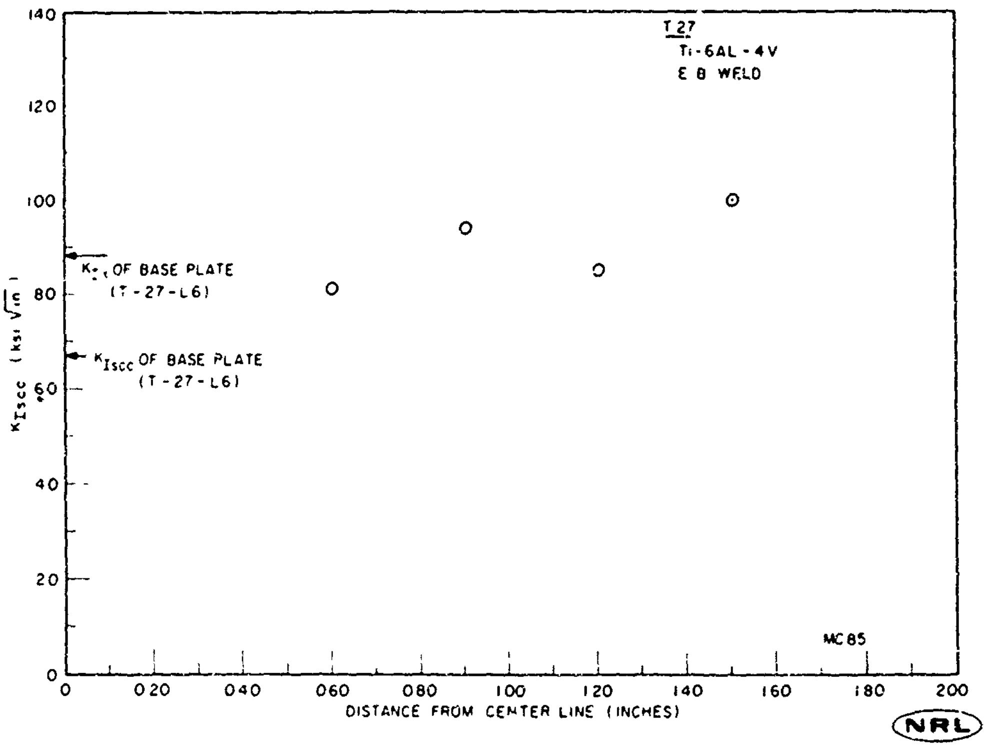

Fig. 79 - Environmental cracking characteristics of an electron beam weldment of titanium alloy T-27

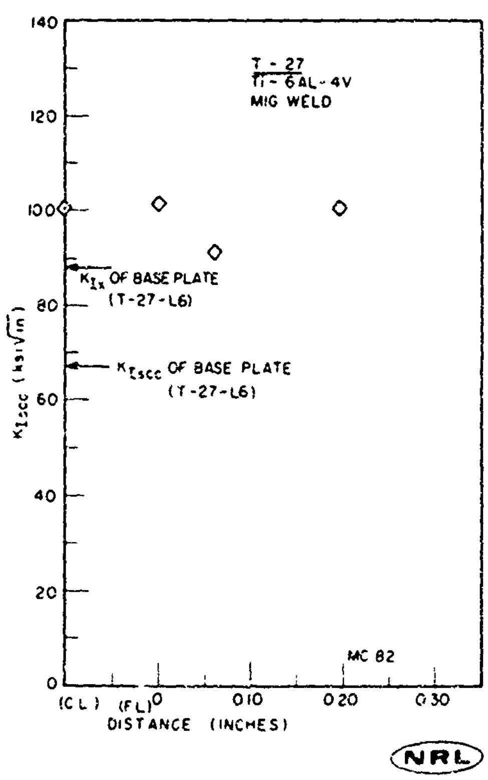

Fig. 80 - Environmental cracking characteristics of a MIG weldment of titanium alloy T-27

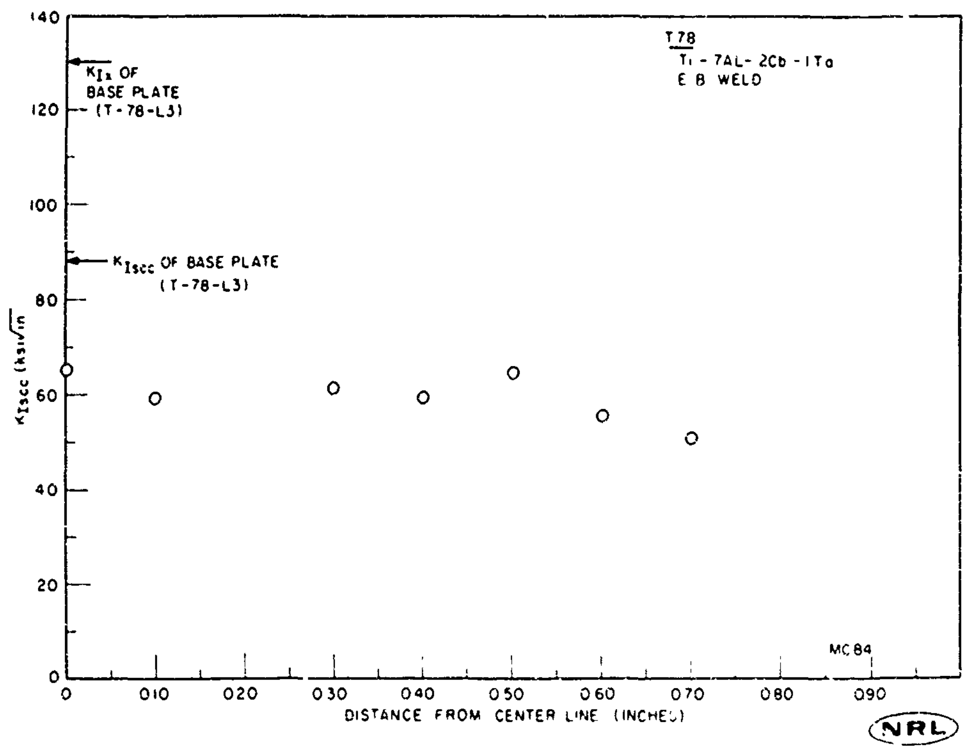

Fig. 81 - Environmental cracking characteristics of an electron beam weldment of titanium alloy T-78

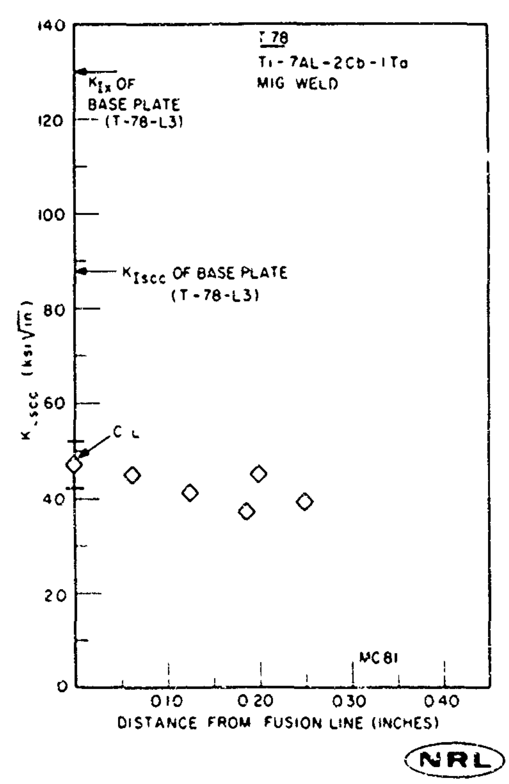

Fig. 82 - Environmental cracking characteristics of a MIG weldment of titanium alloy T-78

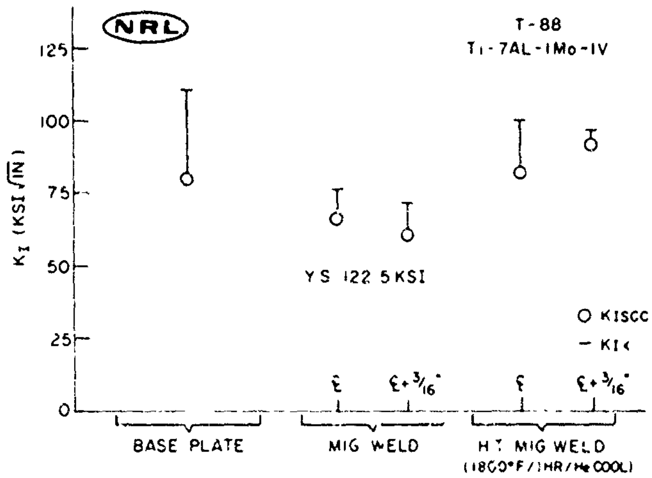

Fig. 83 - Environmental cracking characteristics of a MIG weldment of titanium alloy T-88 both as welded and solution heat treated

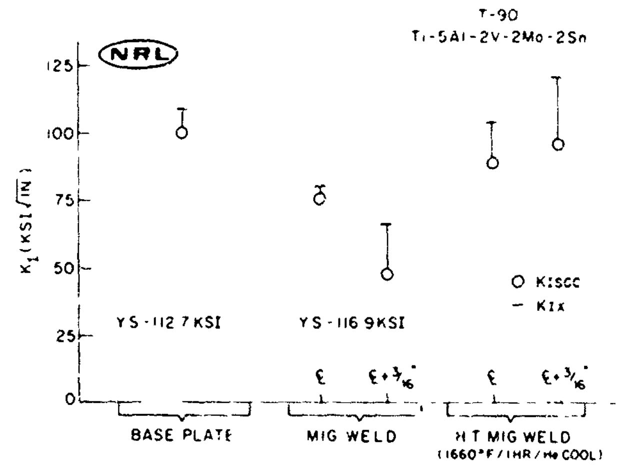

Fig. 84 - Environmental cracking characteristics of a MIG weldment of titanium alloy T-90

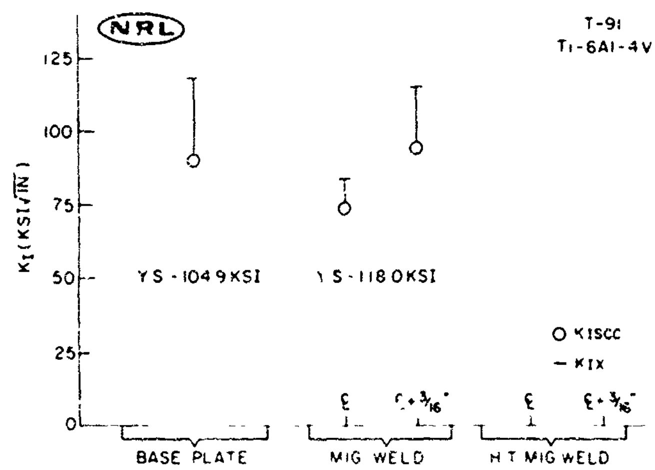

Fig. 85 - Environmental cracking characteristics of a MIG weldment of titanium alloy T-91 (as welded)

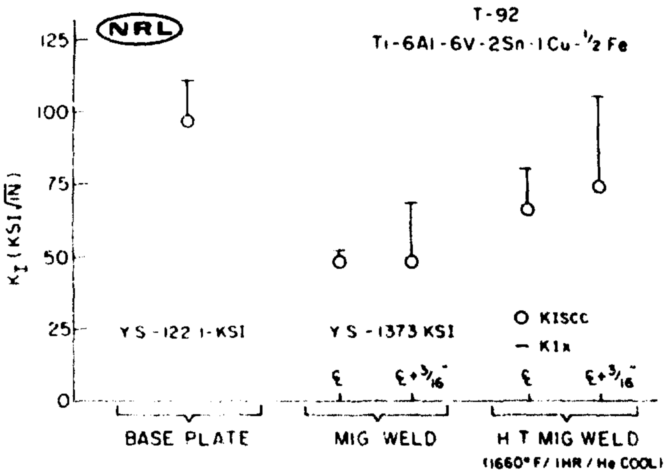

Fig. 86 - Environmental cracking characteristics of a MIG weldment of titanium alloy T-92

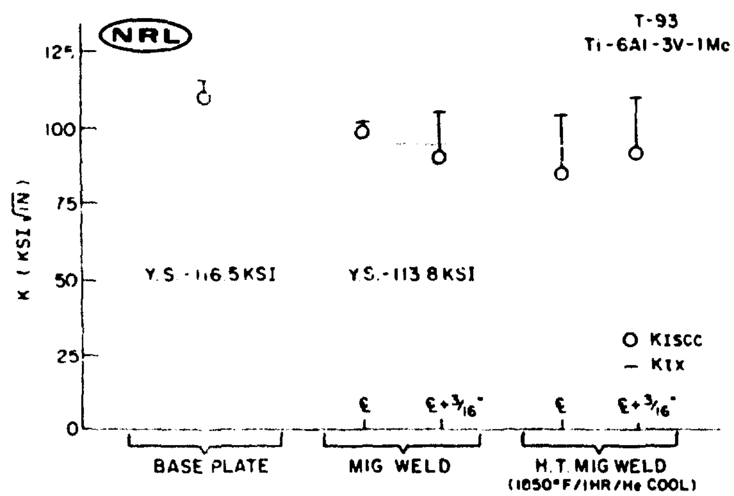

Fig. 87 - Environmental cracking characteristics of a MIG weldment of titanium alloy T-93

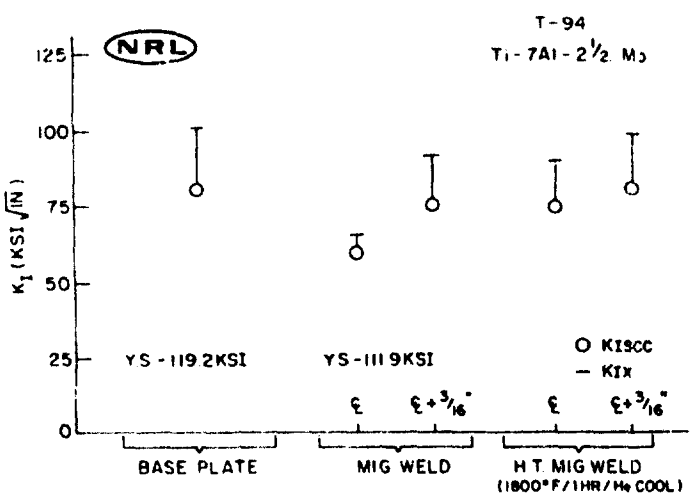

Fig. 88 - Environmental cracking characteristics of a MIG weldment of titanium alloy T-94

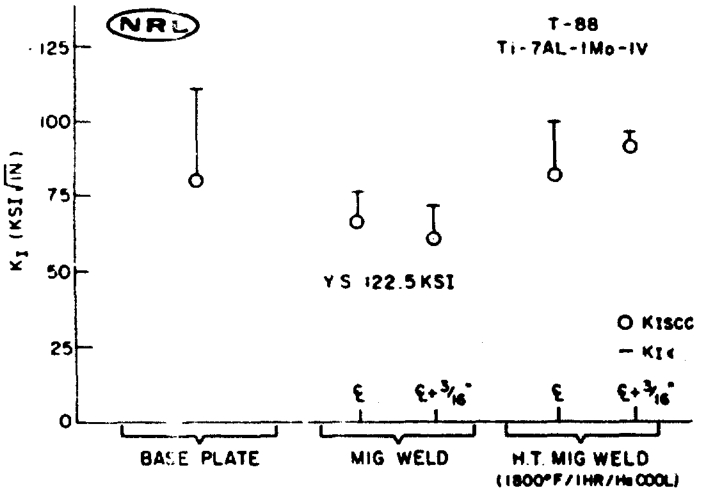

Fig. 83 - Environmental cracking characteristics of a MIG weldment of titanium alloy T-88 both as welded and solution heat treated

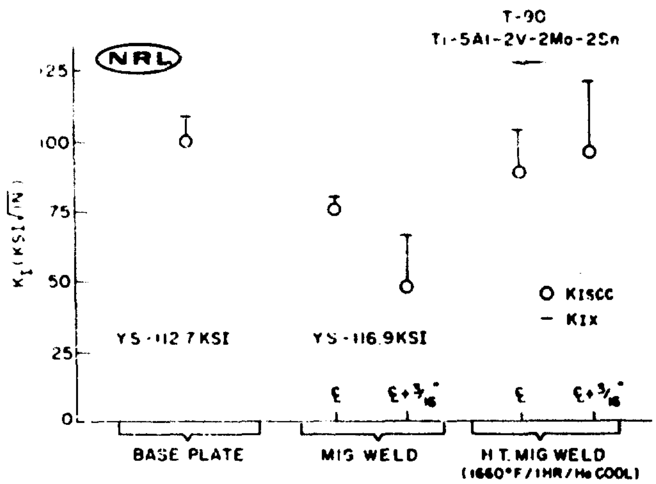

Fig. 84 - Environmental cracking characteristics of a MIG weldment of titanium alloy T-90

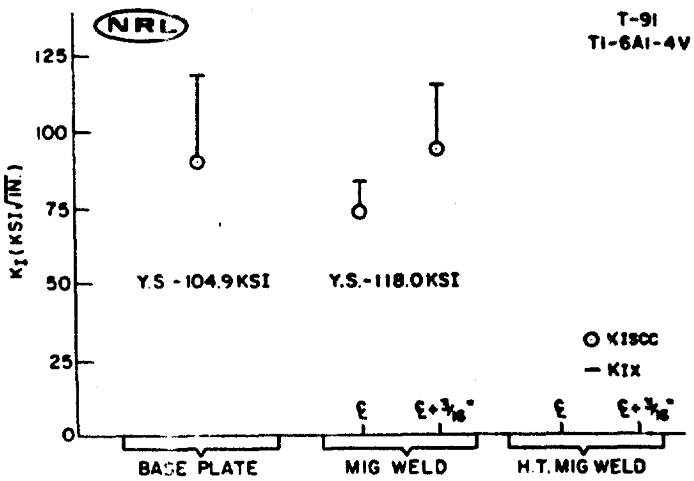

Fig. 85 - Environmental cracking characteristics of a MIG weldment of titanium alloy T-91 (as welded)

UNCLASSIFIED

Security Classification

DOCUMENT CONTROL DATA - R & D

(Security classification of title, body of abstract and indexing annotation must be entered when the overall report is classified)

1. ORIGINATING ACTIVITY (Corporate author) Naval Research Laboratory Washington, D.C. 20390	2a. REPORT SECURITY CLASSIFICATION Unclassified 2b. GROUP

3. REPORT TITLE

STRESS-CORROSION CRACKING CHARACTERISTICS OF ALLOYS OF TITANIUM IN SALT WATER

4. DESCRIPTIVE NOTES (Type of report and inclusive dates)

This is an interim report; work is continuing.

5. AUTHOR(S) (First name, middle initial, last name)

R. W. Judy, Jr. and R. J. Goode

6. REPORT DATE	7a. TOTAL NO. OF PAGES	7b. NO. OF REFS
July 21, 1967	48	6

8a. CONTRACT OR GRANT NO. NRL Problems F01-17 and M04-08B NONR-610(09), NONR-760(31), and N00014-66-C0365 b. PROJECT NO. SP-01426 c. ARPA Order No. 878 d.	9a. ORIGINATOR'S REPORT NUMBER(S) NRL Report 6564 9b. OTHER REPORT NO(S) (Any other numbers that may be assigned this report)

10. DISTRIBUTION STATEMENT

Distribution of this document is unlimited.

11. SUPPLEMENTARY NOTES	12. SPONSORING MILITARY ACTIVITY Department of the Navy (Naval Ship Systems Command), Washington, D. C. 20360 and Advanced Research Projects Agency, Washington, D. C. 20301

13. ABSTRACT

The salt water stress-corrosion cracking (SCC) characteristics have been determined for a large number of titanium alloys representatives of commercial production. These data were compiled as part of an NRL program directed to determining the underlying principles of SCC in metals and to establishing procedures for improving the SCC resistance of these metals as well as learning to tolerate the problem where it exists.

The SCC resistance was determined using a precracked cantilever bend specimen with analysis by fracture mechanics techniques. The test results for the spectrum of alloys and weldments studied indicate that no correlation with mechanical properties exists, which makes precise prediction of SCC properties of particular alloys difficult, if not impossible.

The data obtained provide guideline information for programs similar in nature to the NRL program as well as for alloy development, design and materials selection, and specifications and quality control.

DD FORM 1473

UNCLASSIFIED

Security Classification

UNCLASSIFIED
Security Classification

14. KEY WORDS	LINK A		LINK B		LINK C	
	ROLE	WT	ROLE	WT	ROLE	WT
Stress-corrosion cracking Titanium alloys Weldments						

DD FORM 1 NOV 65 1473 (BACK) GPO 978-633
(PAGE 2)

UNCLASSIFIED
Security Classification